

# Optimized Profiles for Astigmatic Refractive Surgery

Samuel Arba-Mosquera<sup>1,2</sup>, Sara Padroni<sup>3</sup>,  
Sai Kolli<sup>4</sup> and Ioannis M. Aslanides<sup>3</sup>

<sup>1</sup>*Grupo de Investigación de Cirugía Refractiva y Calidad de Visión, Instituto de Oftalmobiología Aplicada, University of Valladolid, Valladolid,*

<sup>2</sup>*SCHWIND eye-tech-solutions, Kleinostheim,*

<sup>3</sup>*Emmetropia Mediterranean Eye Clinic, Heraklion,*

<sup>4</sup>*Moorfields Eye Hospital, London,*

<sup>1</sup>*Spain*

<sup>2</sup>*Germany*

<sup>3</sup>*Greece*

<sup>4</sup>*United Kingdom*

## 1. Introduction

For the correction of astigmatism, many different approaches have been tested, with different degrees of success, through the years<sup>1</sup>. Patient satisfaction in any refractive surgery, wavefront-guided or not, is primarily dependent on successful treatment of the lower order aberrations (LOA) of the eye (sphere and cylinder). Achieving accurate clinical outcomes and reducing the likelihood of a retreatment procedure are major goals of refractive surgery. LASIK has been successfully used for low to moderate myopic astigmatism, whether LASIK is acceptably efficacious, predictable, and safe in correcting higher myopic astigmatism is less documented, especially with regard to the effects of astigmatic corrections in HOA's.

The correction of astigmatism has been approached using several techniques and ablation profiles. There are several reports showing good results for compound myopic astigmatism using photorefractive keratectomy (PRK) and LASIK, but ablation profiles usually cause a hyperopic shift because of a coupling effect in the flattest corneal meridian. A likely mechanism of this coupling effect is probably due to epithelial remodeling and other effects such as smoothing by the LASIK flap. In cases of large preoperative amounts of astigmatism, deviations from the target refractive outcome are usually attributed to "coupling factors." Nevertheless, the investigation of the coupling factor remains a rather difficult task, because it seems to be dependent on various factors. Individual excimer laser systems may have different coupling factors, cutting the flap could alter the initial prescription and different preoperative corneal curvatures (K-reading) may have influence on coupling factor.

## 2. Induction of aberrations

While for quasi-spherical corrections the focus has been moved from primary refractive outcomes to effects of the ablation in postoperative high order aberrations (HOA)<sup>5,38,28</sup>, for

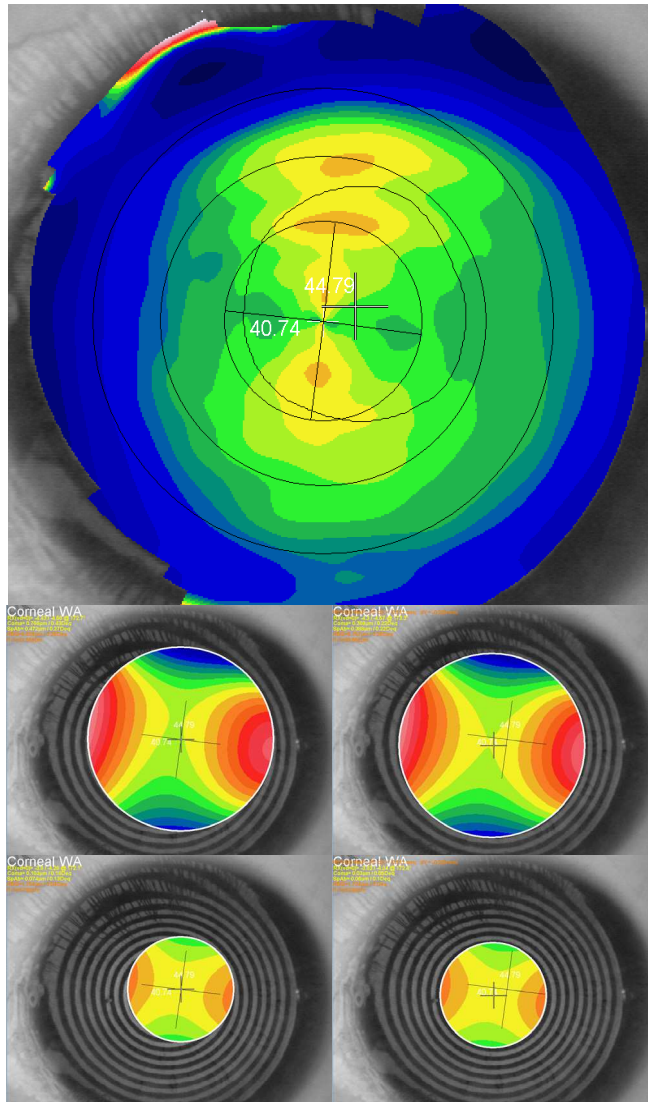


Fig. 1. Representations of the astigmatic error. Top: Topographic astigmatism measured at the corneal vertex within the central 3mm disc showing 4D of astigmatism. Middle left: 7mm diameter wavefront irregular astigmatism measured at the pupil centre showing 4.6D regular astigmatism with 0.4D coma and 0.3D spherical aberration. Middle right: 7mm diameter wavefront more regular astigmatism measured at the corneal vertex showing 4.6D regular astigmatism with only 0.2D coma and 0.2D spherical aberration. Bottom left: 4mm diameter refractive irregular astigmatism measured at the pupil centre showing 4.25D regular astigmatism with 0.2D coma and 0.1D spherical aberration. Bottom right: 4mm diameter refractive more regular astigmatism measured at the corneal vertex showing 4.25D regular astigmatism with 0D coma and 0.1D spherical aberration.

astigmatism the focus mainly remained at the primary refractive outcomes, principally due to the encountered problems as “coupling factors”<sup>5</sup> or cyclotorsion errors<sup>38</sup>, which result in residual astigmatism.

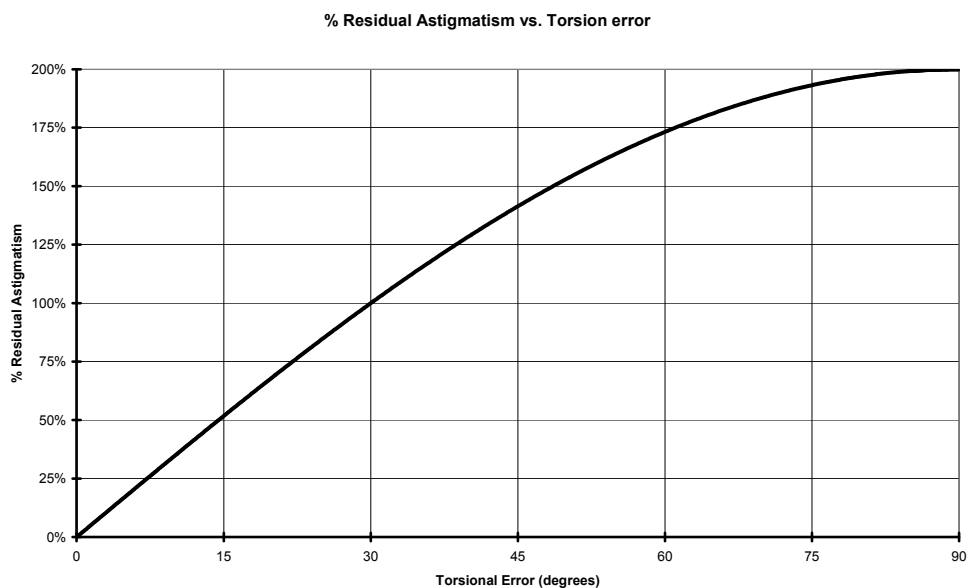


Fig. 2. Residual astigmatism magnitude vs. torsion error (assuming the astigmatic error and the correcting cylinder are at the same plane and are equal in dioptric power).

Refractive surgeons have been observing post-operatively a resulting hyperopic refraction on the sphere (hyperopic shift) whenever they applied a negative cylinder onto the cornea.

This output sphere was not planned and depends on several factors:

- Variation for different refractive LASER systems
- Dependant on the intended negative cylinder in a non-linear relation
- Changing for sphero-cylindrical correction compared to pure cylindrical ones

Due to all these reasons, it was an issue for the surgeons to properly include this effect in their nomograms to achieve the intended refraction.

Most of the LASER manufacturers and surgeons used the “Coupling Factor”<sup>2</sup> defined as the averaged output sphere per single diopter of pure negative cylinder achieved.

Despite of its empirical nature, this Coupling Factor allows the surgeon to plan the treatment with reasonable success.

The hint for one of the sources of this “coupling effect” was the analysis of a pure negative cylinder case. When a pure negative cylinder is applied, the neutral axis becomes refractive, being deeper at the centre compare to the periphery.

The “Coupling Factor” is a nomogram-like “adjustment” introduced by surgeons to achieve the intended result. With the introduction of Wavefront guided ablation volumes and loss of efficiency compensation factors; these effects should be mainly compensated in the devices by refined algorithms instead of nomogrammed by the surgeon.

The currently available methods allow for the correction of refractive include astigmatism<sup>3</sup> defects. One of the unintended effects induced by laser surgery is the induction of aberrations, which causes halos and reduced contrast sensitivity<sup>4</sup>. The loss of ablation efficiency at non-normal incidence can explain, in part, many of these unwanted effects, such as induction of high order astigmatism of postoperative corneas after myopic surgery. Considering a loss of efficiency model applied to a simple myopic astigmatism profile, the neutral axis becomes refractive, being less ablated in the periphery as compared to the centre, whereas the refractive axis “shrinks,” steepening the curvature and then slightly increasing the myopic power of the axis as well as inducing aberrations. The net effect can be expressed as an unintended myopic ablation (hyperopic shift), and a small undercorrection of the astigmatic component.

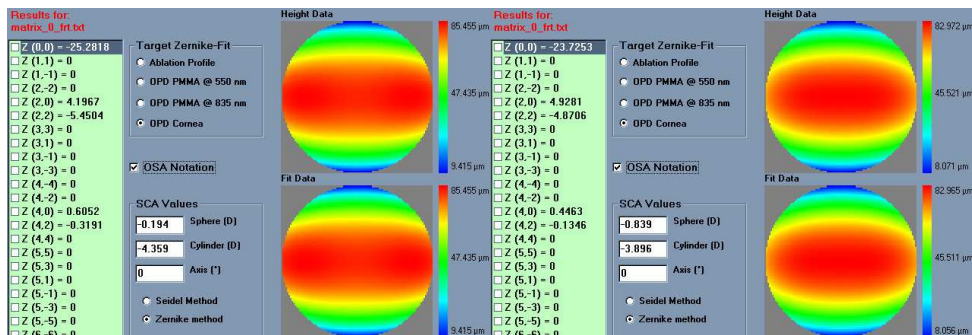


Fig. 3. Effect of the hyperopic shift and coupling factor in the ablative refractive correction. Left: attempted correction. Right: simulated correction considering uncompensated reflection, projection, and geometric efficiency losses. Notice that an unintended -0.75D extra myopic spherical correction is induced, and a reduction of 0.5D in the astigmatic correction.

Several models have been proposed to compensate for those effects.

The models by Arba-Mosquera&de-Ortueta<sup>5</sup> provide a general method to analyze the loss of ablation efficiency at non-normal incidence in a geometrical way. The model is comprehensive and directly considers curvature, system geometry, applied correction, and astigmatism as model parameters, and indirectly laser beam characteristics and ablative spot properties. The model replaces the direct dependency on the fluence by a direct dependence on the nominal spot volume and on considerations about the area illuminated by the beam, reducing the analysis to pure geometry of impact. Compensation of the loss of ablation efficiency at non-normal incidence can be made at relatively low cost and would directly improve the quality of results.

The proposed models provide results essentially identical to those obtained with the model by Dorransoro-Cano-Merayo-Marcos<sup>5</sup>. Additionally, it offers an analytical expression including some parameters that were ignored (or at least not directly addressed) in previous analytical approaches.

Different effects interact; the beam is compressed due to the loss of efficiency, but at the same time expands due to the angular “projection.” Losses of ablation efficiency at non-normal incidence in refractive surgery, may explain up to 45% of the reported increase in

aberrations. The loss of efficiency is an effect that should be offset in commercial laser systems using sophisticated algorithms that cover most of the possible variables. Parallel to the clinical developments, increasingly capable, reliable, and safer laser systems with better resolution and accuracy are required.

Corneal curvature and applied correction play an important role in the determination of the ablation efficiency and are taken into account for accurate results. However, corneal toricity and applied astigmatism do not have a relevant impact as long as their values correspond to those of normal corneas. Only when toricity or astigmatism exceeds 3 D, their effects on ablation efficiency start to be significant. Surface asphericity showed minor effects.

The loss of efficiency in the ablation and non-normal incidence are responsible for much of the induction of aberrations observed in the treatments as well as many undercorrections observed in astigmatism with major implications for treatment and optical outcome of the procedure. Compensation can be made at relatively low cost and directly affects the quality of results.

Considering this model of loss of efficiency, we have applied it for different LASER peak radiant exposures (FWHM 1mm, Gaussian profile), then we have calculated the "Coupling Factor" according to the averaged output sphere per single diopter of pure negative cylinder achieved.

Peak Radiant Exposure (mJ/cm <sup>2</sup> )	Coupling Factor (%)
100	37
130	22
180	16
230	11
300	8
400	5

Table 1. Theoretical coupling factor as a function of the laser fluence.

Today, several approaches to import, visualize, and analyze high detailed diagnostic data of the eye (corneal or ocular wavefront data) are offered. At the same time, several systems are available to link diagnostic systems for measurement of corneal and ocular aberrations<sup>6</sup> of the eye to refractive laser platforms. These systems are state-of-the-art with flying spot technology, high repetition rates, fast active eye trackers, and narrow beam profiles. Consequently, these systems offer new and more advanced ablation capabilities, which may potentially suffer from new sources of "coupling" (different Zernike orders<sup>5</sup> affecting each other with impact on the result). The improper use of a model that overestimates or underestimates the loss of efficiency will overestimate or underestimate its compensation and will only mask the induction of aberrations under the appearance of other sources of error.

In coming years, the research and development of algorithms will continue on several fronts in the quest for zero aberration. This includes identification of sources for induction of aberrations, development and refinement of models describing the pre-, peri- and postoperative biomechanics of the cornea, development of aberration-free profiles leaving pre-existing aberrations of the eye unchanged, redevelopment of ablation profiles to

compensate for symptomatic aberrated eyes in order to achieve an overall postoperative zero level of aberration (corneal or ocular)<sup>7</sup>. Finally, the optimal surgical technique (LASIK (Laser assisted in-situ Keratomileusis), LASEK (Laser Epithelial Keratomileusis), PRK (Photorefractive Keratectomy), Epi-LASIK ...) to minimize the induction of aberrations to a noise level has not yet been determined<sup>8</sup>.

### 3. Baseline for refractive profiles

When a patient is selected for non-customized aspherical treatment, the global aim of the surgeon should be to leave all existing high-order-aberrations (HOA) unchanged because the best-corrected visual acuity, in this patient, has been unaffected by the pre-existing aberrations. Hence, all factors that may induce HOAs, such as biomechanics, need to be taken into account prior to the treatment to ensure that the preoperative HOAs are unchanged after treatment<sup>38</sup>.

Then, in the treatments, the goals should be:

- For aspherical treatments: no induced aberrations; a change in asphericity depending on the corrected defocus.
- For wavefront-guided treatments: change in aberrations according to diagnosis; change in asphericity depending on the corrected defocus and on the  $C(n,0)$  coefficients applied.

Even though the condition of stigmatism, that origins "free of aberration" verified for two points (object and image) and for a conicoid under limited conditions, is very sensitive to

	Aberration-free Treatment	Corneal Wavefront Treatment	Ocular Wavefront Treatment
Aspheric ablation profile	Yes	Yes	Yes
Bi-aspheric ablation profile for the correction of Presbyopia	Using PresbyMAX	Using PresbyMAX	Using PresbyMAX
Simultaneous correction of Sphere + Cylinder	Yes	Yes	Yes
Correction of high order aberrations (HOA)	Preserved	Yes	Yes
Compensation by microkeratome usually induced aberrations (biomechanical effect)	Yes	Yes	Yes
Compensation of ablation induced aberrations (biomechanical effect)	Yes	Yes	Yes
Compensation of energy loss of the laser beam	Yes	Yes	Yes

Table 2. Level of detail of the treatment approaches considered at the AMARIS system.

small deviations and decentrations (a question that usually arises in refractive surgery), the goal of these profiles is not to achieve an stigmatism condition postoperatively, but rather to maintain the original HO wavefront-aberration.

The optical quality in an individual can be maximized for a given wavelength and a given distance by canceling the aberration of his wavefront and optimizing his defocus (for a single distance), but this has direct implications dramatically negative for the optical quality for the rest of wavelengths (greater negative effect the more extreme is the wavelength). However, the optical quality of a person showing a certain degree of aberration of his wavefront decreases compared to the maximum obtainable in the absence of aberration, but it has direct positive implications in the "stability" of the optical quality for a wide range for wavelengths (which covers the spectral sensitivity of the human eye)<sup>9</sup> and in the depth of focus, i.e. for a range of distances that can be considered "in-focus" simultaneously. Lastly, moderate levels of wavefront-aberration favor the stability of the image quality for wider visual fields<sup>10</sup>. In such a way, there are, at least, three criteria (chromatic blur, depth of focus, wide field vision) favoring the target of leaving minor amounts of not clinically relevant aberrations (the proposed "aberration-free" concept).

With simple spherical error, degradation of resolution begins for most people with errors of 0.25 D. A similar measure can be placed on the error due to cylinder axis error.

Optimized patterns for refractive surgery aiming to be neutral for aberrations together with the consideration of other sources of aberrations such as blending zones, eye-tracking, and corneal biomechanics having close-to-ideal ablation profiles should improve the clinical results decreasing the need for nomograms, and reducing the induced aberrations after surgery.

#### 4. The astigmatic refraction problem

Classical ametropias (myopia, hyperopia and astigmatism) are, similarly to aberration errors, differences to a reference surface, and are included in the, more general, wavefront error. However, classical ametropias are used to be described, not in units of length, but in units of optical refractive power.

It is, then, necessary to find a relationship between wavefront error magnitudes and classical ametropias<sup>11,12,13,14,15</sup>. This relationship is often called "objective wavefront refraction":

The quadratic equivalent of a wave-aberration map can be used as a relationship between wavefront-error magnitudes and classical ametropias. That quadratic is a sphero-cylindrical surface, which approximates the wave aberration map. The idea of approximating an arbitrary surface with a quadratic equivalent is a simple extension of the ophthalmic technique of approximating a sphero-cylindrical surface with an equivalent sphere.

Several possibilities to define this relationship can be found in the literature:

- Objective wavefront refraction from low order Zernike modes at full pupil size<sup>16</sup>
- Objective wavefront refraction from Seidel aberrations at full pupil size<sup>16</sup>
- Objective wavefront refraction from low order Zernike modes at subpupil size<sup>16</sup>
- Objective wavefront refraction from Seidel aberrations at subpupil size<sup>16</sup>
- Objective wavefront refraction from paraxial curvature
- Objective wavefront refraction from wavefront axial refraction<sup>17</sup>
- Wavefront refraction from low order Zernike modes at full pupil size

A common way to fit an arbitrarily aberrated wavefront with a quadratic surface is to find the surface that minimizes the sum of the squared deviations between the two surfaces.

The least-square fitting method is the basis of the Zernike wavefront expansion. Since the Zernike expansion employs an orthogonal set of basic functions, the least-square solution is simply given by the second-order Zernike coefficients of the aberrated wavefront, regardless of the values of the other coefficients. These second-order Zernike coefficients can be converted into a sphero-cylindrical prescription in power vector notation of the form [J<sub>0</sub>, M, J<sub>45</sub>].

$$J_0 = \frac{-8\sqrt{6}C_2^{+2}}{PD^2} \quad (1)$$

$$M = \frac{-16\sqrt{3}C_2^0}{PD^2} \quad (2)$$

$$J_{45} = \frac{-8\sqrt{6}C_2^{-2}}{PD^2} \quad (3)$$

where PD is the pupil diameter, M is the spherical equivalent, J<sub>0</sub>, the cardinal astigmatism and J<sub>45</sub> the oblique astigmatism. The components J<sub>0</sub>, M, and J<sub>45</sub> represent the power of a Jackson crossed cylinder with axes at 0 and 90°, the spherical equivalent power, and the power of a Jackson crossed cylinder with axes at 45 and 135°, respectively.

The power-vector notation is a cross-cylinder convention that is easily transposed into conventional refractions in terms of sphere, cylinder, and axis in the minus-cylinder or plus-cylinder formats used by clinicians.

$$S = M - \frac{C}{2} \quad (4)$$

$$C = 2\sqrt{J_0^2 + J_{45}^2} \quad (5)$$

$$A = \frac{\arctan\left(\frac{J_{45}}{J_0}\right)}{2} \quad (6)$$

- Objective wavefront refraction from Seidel aberrations at full pupil size

The Seidel sphere adds a value for the primary spherical aberration to improve, in theory, the fit of the wavefront to a sphere and improve accuracy of the spherical equivalent power.

$$M = \frac{-16\sqrt{3}C_2^0 + 48\sqrt{5}C_4^0}{PD^2} \quad (7)$$

- Objective wavefront refraction from low order Zernike modes at subpupil size

The same low-order Zernike modes can be used to calculate the refraction for any given smaller pupil size, either by refitting the raw wave-aberration data to a smaller diameter, or by mathematically performing the so-called radius transformation<sup>18</sup> of the Zernike expansion to a smaller diameter.



- Objective wavefront refraction from Seidel aberrations at subpupil size  
In the same way, Seidel aberrations can be used to calculate the refraction for any subpupil size.

- Objective wavefront refraction from paraxial curvature  
Curvature is the property of wavefronts that determines how they focus. Thus, another reasonable way to fit an arbitrary wavefront with a quadratic surface is to match the curvature of the two surfaces at some reference point.

A variety of reference points could be selected, but the natural choice is the pupil center. Two surfaces that are tangent at a point and have the same curvature in every meridian are said to osculate. Thus, the surface we seek is the osculating quadric.

Fortunately, a closed-form solution exists for the problem of deriving the power vector parameters of the osculating quadratic from the Zernike coefficients of the wavefront. This solution is obtained by computing the curvature at the origin of the Zernike expansion of the Seidel formulae for defocus and astigmatism. This process effectively collects all  $r^2$  terms from the various Zernike modes.

$$J_0 = \frac{-8\sqrt{6}C_2^{-2} + 24\sqrt{10}C_4^{-2} - 48\sqrt{14}C_6^{-2} + 240\sqrt{2}C_8^{-2} - 120\sqrt{22}C_{10}^{-2} + \dots}{PD^2} \tag{8}$$

$$M = \frac{-16\sqrt{3}C_2^0 + 48\sqrt{5}C_4^0 - 96\sqrt{7}C_6^0 + 480C_8^0 - 240\sqrt{11}C_{10}^0 + \dots}{PD^2} \tag{9}$$

$$J_{45} = \frac{-8\sqrt{6}C_2^{+2} + 24\sqrt{10}C_4^{+2} - 48\sqrt{14}C_6^{+2} + 240\sqrt{2}C_8^{+2} - 120\sqrt{22}C_{10}^{+2} + \dots}{PD^2} \tag{10}$$

- Objective wavefront refraction from wavefront axial refraction  
It is also possible to represent the wavefront aberration in optical refractive power, without the need of simplifying it to a quadric surface, and, therefore, providing a higher level of detail. Straightforward approach for the problem is to use the concept of axial refractive error (vergence maps<sup>19</sup>) (Fig. 4).

The line of sight represents a chief ray; the wavefront aberration is zero at the pupil centre, and perpendicular to the line of sight. Each point of the wavefront propagates perpendicular to the local surface of the wavefront. The axial distance from the pupil centre to the intercept between the propagated local wavefront and the line of sight expressed in dioptres corresponds to the axial refractive error.

$$ARx(\rho, \theta) = \frac{-1}{r} \frac{\partial W(\rho, \theta)}{\partial \rho} \tag{11}$$

A schematic comparison of the different quadric methods described here for the determination of the objective wavefront refraction for a given pupil size is depicted in Fig. 5.

- Automatic Manifest Refraction Balance  
These objective methods for calculating the refraction are optically correct but have some practical limitations in clinical practice<sup>20,21</sup>.  
The devices to obtain the wavefront aberration of an eye use to work in the infrared range (IR), which is invisible for the human eye and avoid undesired miotic effects in the pupil

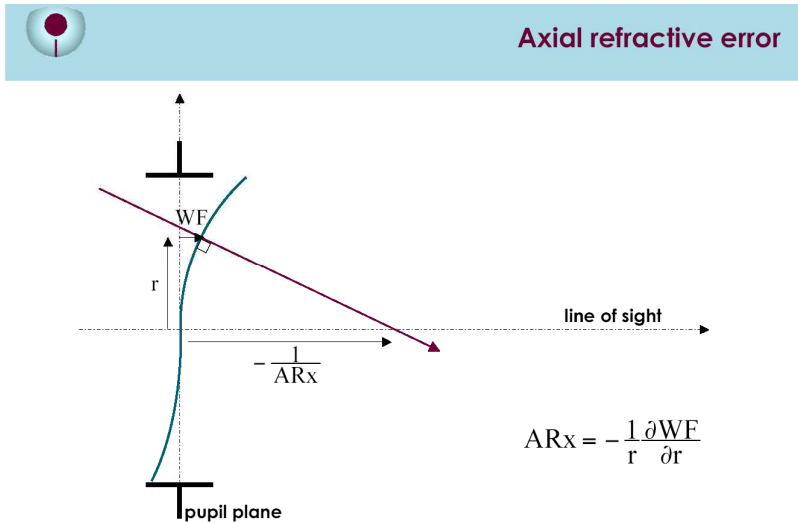


Fig. 4. Representation of the axial refractive error. The line of sight represents a chief ray; the wavefront aberration is zero at the pupil centre, and perpendicular to the line of sight. Each point of the wavefront propagates perpendicular to the local surface of the wavefront. The axial distance from the pupil centre to the intercept between the propagated local wavefront and the line of sight expressed in dioptres corresponds to the axial refractive error<sup>17</sup>.

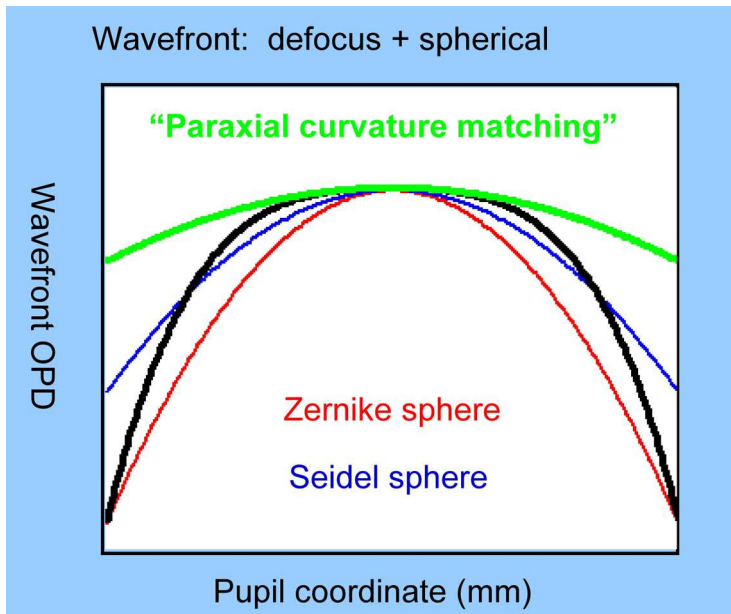


Fig. 5. Comparison of the different quadric methods described here for the determination of the objective wavefront refraction for a given pupil size.

size. The refractive indices of the different optical elements in our visual system depend on the wavelength of the illumination light. In this way, the propagated wavefront (and the corresponding wavefront aberration) ingoing to (or outcoming from) our visual system depends on the wavelength of the illumination light, leading to the so-called chromatic aberration<sup>22</sup>.

The different methods provide “slightly” different results, depending on how they are compared to the subjective manifest refraction, one or another correlates better with manifest refraction<sup>16</sup>.

HOAb influence LOAb (refraction) when analysed for smaller diameters: For full pupil (e.g. 6 mm) the eye sees the world through HOAb producing some multifocality but without defocus, for a smaller pupil (e.g. 4 mm), the optical aberration of the eye is the same but the outer ring is blocked, thereby the eye sees the world through the central part of the HOAb, which may produce some defocus or astigmatism (LOAb, refraction).

A variation of the objective wavefront refraction from low-order Zernike modes at a fixed subpupil diameter of 4 mm was chosen as starting point to objectively include the measured subjective manifest refraction in the wave aberration (Fig. 6 to Fig. 9).

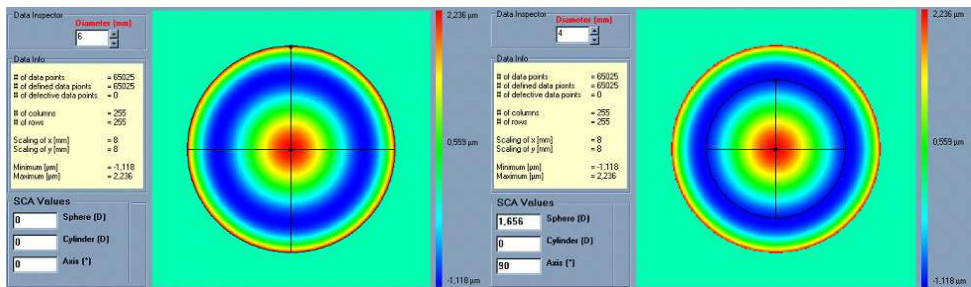


Fig. 6. Zernike refraction of a pure Spherical Aberration (at 6 mm) is per definition 0 because Spherical Aberration is a High Order Aberration mode, when analysed for a smaller diameter (4 mm) produces Defocus.

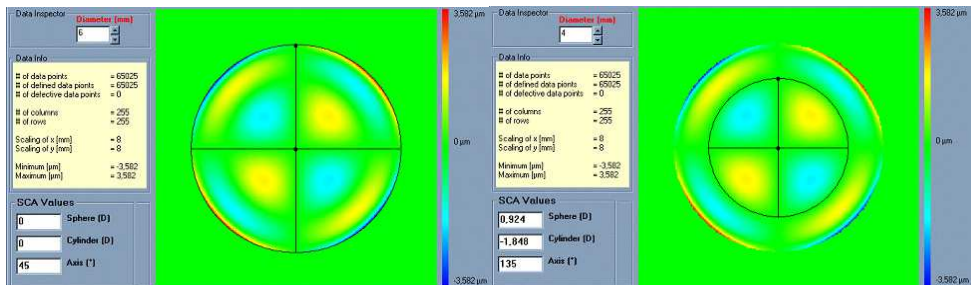


Fig. 7. Zernike refraction of a pure High Order Astigmatism (at 6 mm) is per definition 0 because of High Order Aberration mode, when analysed for a smaller diameter (4 mm) produces Astigmatism.

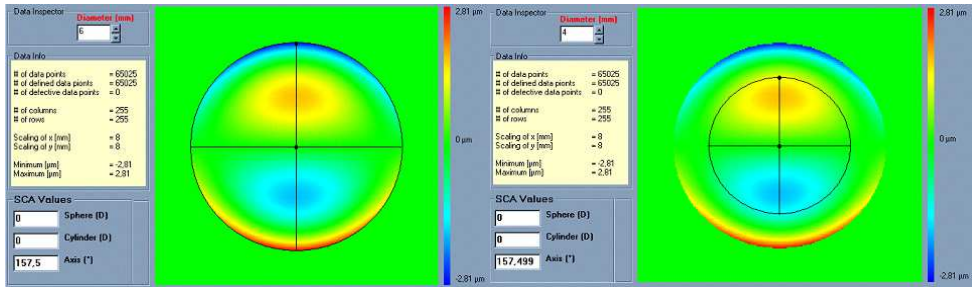


Fig. 8. Zernike refraction of a pure Coma (at 6 mm) is per definition 0 because Coma is a High Order Aberration mode, when analysed for a smaller diameter (4 mm) produces only tilt. Notice that coma may have “visual effect” if the visual axis changes producing Astigmatism.

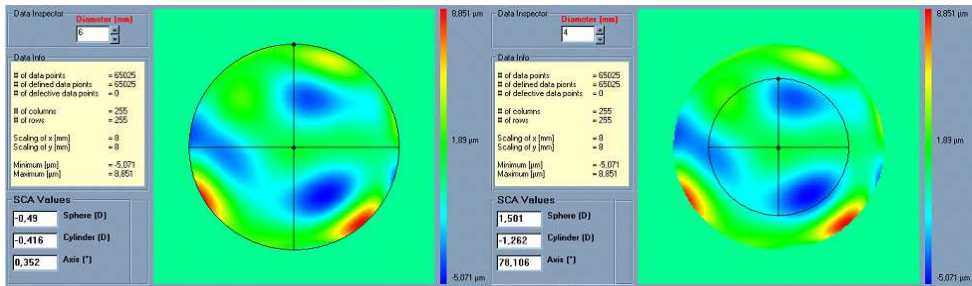


Fig. 9. Zernike refraction of a general wavefront aberration analysed at 6 mm and analysed for a smaller diameter (4 mm).

The expected optical impact of high-order aberrations in the refraction is calculated and modified from the input manifest refraction. The same wave aberration is analysed for two different diameters: for the full wavefront area (6 mm in this study) and for a fixed subpupil diameter of 4 mm. The difference in refraction obtained for each of the two diameters corresponds to the manifest refraction associated to the high-order aberrations (Fig. 10).

The condition is to re-obtain the input manifest refraction for the subpupil diameter of 4 mm. This way, the low-order parabolic terms of the modified wave aberration for the full wavefront area can be determined.

- Comprehensive astigmatism planning and analysis

**Step 1.** (Common) Calculation of the correction at the corneal plane

We first recalculate the correction components from the spectacle plane to the corneal plane where the ablation will take place:

$$S_{CP} = \frac{S_{SP}}{1 - S_{SP}VD} \tag{12}$$

Where  $S_{CP}$  is the spherical component at corneal plane,  $S_{SP}$  is the spherical component at spectacle plane and  $VD$  the vertex distance from the corneal plane to the spectacle plane.

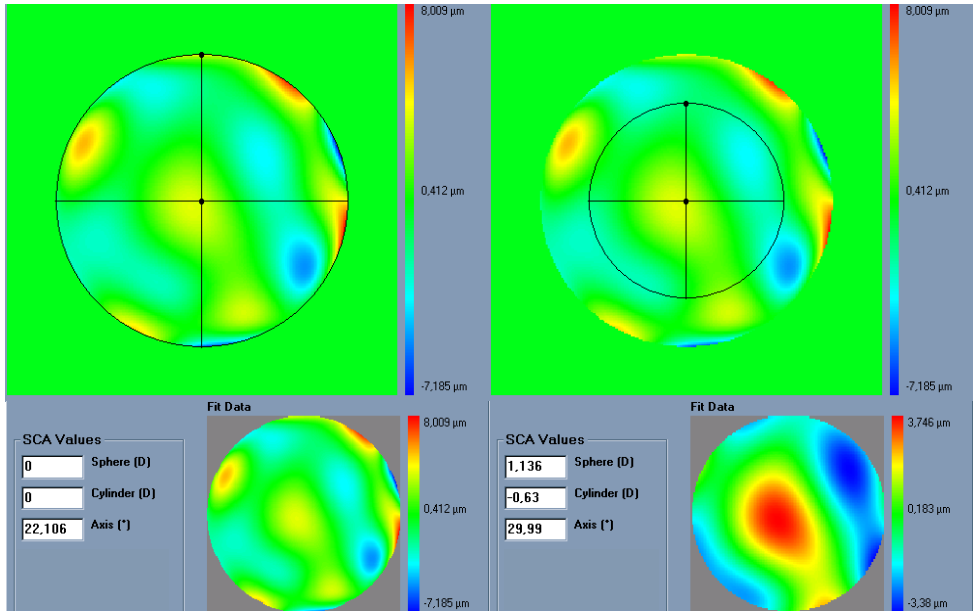


Fig. 10. Automatic Refraction Balance. Optical impact of the HOAb the refraction is calculated and balanced from input refraction. Notice that the same wavefront aberration is analysed for two different diameters. The difference in the refraction provided at the two different analysis diameters correspond to the manifest refraction provided by the high order aberration.

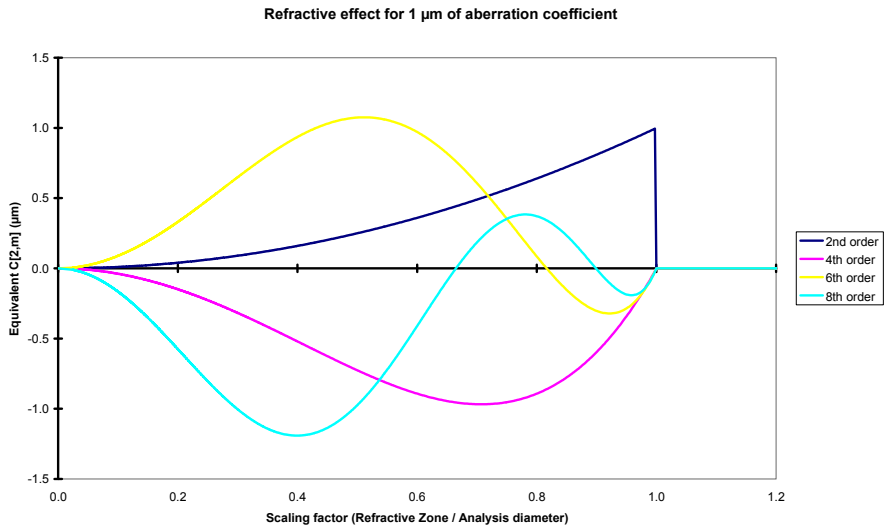


Fig. 11. Refractive effect of 1 $\mu$ m aberration as a function of the scaling factor from the analysis diameter to the considered refractive zone.

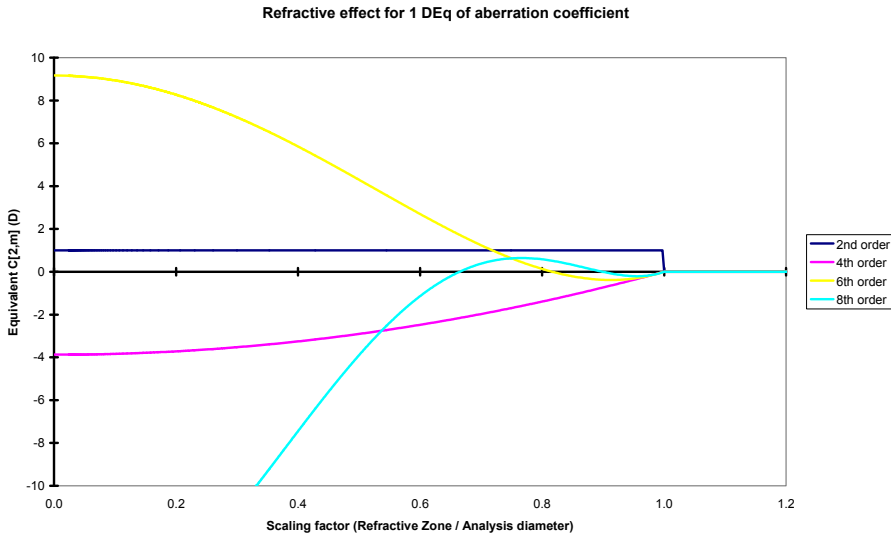


Fig. 12. Refractive effect of 1D aberration as a function of the scaling factor from the analysis diameter to the considered refractive zone.

$$C_{CP} = \frac{S_{SP} + C_{SP}}{1 - (S_{SP} + C_{SP})VD} - S_{CP} \tag{13}$$

Where  $C_{CP}$  is the cylindrical component at corneal plane, and  $C_{SP}$  is the cylindrical component at spectacle plane.

**Step 2.** (Common) Correction of the corneal keratometries to anterior corneal surface curvatures

We measured the best-fit keratometry readings (K-readings) of Maloney index.

The different refractive indices used for the topography and the ablation planning (keratometric refractive index 1.3375 for the topographies, and corneal refractive index 1.376 for the ablations) were taken into account.

$$K_{ACS,i} = K_i \frac{n_{Cornea} - n_{Air}}{n_{Topo} - n_{Air}} \tag{14}$$

Where  $K_{ACS,i}$  are the meridional corneal curvatures of the anterior corneal surface,  $K_i$  are the Maloney K-readings of the cornea,  $n_{Cornea}$  is the refractive index of the cornea (1.376),  $n_{Topo}$  is the refractive index used by the topographer (1.3375), and  $n_{Air}$  is the refractive index of the air (1).

$$K_{ACS,i} = K_i \frac{0.376}{0.3375} \tag{15}$$

Thus, a topographical condition e.g. of 41.65 D at 111°, and 41.21 D at 21°, is considered as 46.40 D at 111°, and 45.91 D at 21° anterior corneal surface curvature, due to the different

refractive indices used by the topographer (keratometric refractive index 1.3375) and the actual refractive index of the cornea (1.376).

**Step 3.** (Common) Expressing the correction at the corneal plane in power vector notation. The conventional refractions in terms of sphere, cylinder and axis in minus-cylinder or plus-cylinder formats used by clinicians can be easily converted to a spherocylindrical prescription in power vector notation of the form  $[J_0, M, J_{45}]$ .

The mathematical formulation is:

$$M_{MR} = S_{CP} + \frac{C_{CP}}{2} \quad (16)$$

$$J_{0,MR} = \frac{-C_{CP}}{2} \cos(2A_{MR}) \quad (17)$$

$$J_{45,MR} = \frac{-C_{CP}}{2} \sin(2A_{MR}) \quad (18)$$

Where M is the spherical equivalent of the manifest refraction at corneal plane,  $J_0$  the cardinal astigmatism and  $J_{45}$  the oblique astigmatism. The components  $J_0$ , M, and  $J_{45}$ , respectively, represent the power of a Jackson crossed-cylinder with axes at 0 and 90°, the spherical equivalent power, and the power of a Jackson crossed-cylinder with axes at 45 and 135°.

**Step 4.** (Common) Expressing the corneal curvatures in power vector notation. The conventional corneal curvatures used by clinicians can be easily converted to spherocylindrical corneal curvatures in power vector notation of the form  $[J_0, M, J_{45}]$ . The mathematical formulation is:

$$M_K = \frac{K_1 + K_2}{2} \quad (19)$$

$$J_{0,K} = \frac{K_1 - K_2}{2} \frac{\cos(2A_1) - \cos(2A_2)}{2} \quad (20)$$

$$J_{45,K} = \frac{K_1 - K_2}{2} \frac{\sin(2A_1) - \sin(2A_2)}{2} \quad (21)$$

Where M is the spherical equivalent of the corneal curvatures,  $J_0$  the cardinal astigmatism and  $J_{45}$  the oblique astigmatism.

**Step 5.** (Common) Calculation of the internal astigmatism in power vector notation. The internal astigmatism is the difference between the manifest and the corneal astigmatism.

The mathematical formulation is:

$$J_{0,I} = J_{0,MR} - J_{0,K} \quad (22)$$

$$J_{45,I} = J_{45,MR} - J_{45,K} \quad (23)$$

**Step 6.** (Common) Calculation of the internal astigmatism in clinician notation

The power vector notation is a cross-cylinder convention that is easily transposed into conventional refractions in terms of cylinder and axis in minus-cylinder or plus-cylinder formats used by clinicians.

$$C_I = 2\sqrt{J_{0,I}^2 + J_{45,I}^2} \quad (24)$$

$$A_I = \frac{\arctan\left(\frac{J_{45,I}}{J_{0,I}}\right)}{2} \quad (25)$$

**Step 7.** (Common) Calculation of the predicted residual manifest refraction in power vector notation

The predicted residual manifest astigmatism is the difference between the planned and the manifest astigmatism.

The mathematical formulation is:

$$J_{0,RM} = J_{0,MR} - J_{0,P} \quad (26)$$

$$J_{45,RM} = J_{45,MR} - J_{45,P} \quad (27)$$

**Step 8.** (Common) Calculation of the predicted residual manifest refraction in clinician notation

The power vector notation is a cross-cylinder convention that is easily transposed into conventional refractions in terms of cylinder and axis in minus-cylinder or plus-cylinder formats used by clinicians.

$$S_{RM,CP} = M_{RM} - \frac{C_{RM,CP}}{2} \quad (28)$$

$$C_{RM,CP} = 2\sqrt{J_{0,RM}^2 + J_{45,RM}^2} \quad (29)$$

$$A_{RM} = \frac{\arctan\left(\frac{J_{45,RM}}{J_{0,RM}}\right)}{2} \quad (30)$$

**Step 9.** (Common) Expressing the predicted residual manifest refraction in clinician notation at spectacle plane

We then recalculate the correction components from the corneal plane to the spectacle plane:

$$S_{RM,SP} = \frac{S_{RM,CP}}{1 + S_{RM,CP}VD} \quad (31)$$



$$C_{RM,SP} = \frac{S_{RM,CP} + C_{RM,CP}}{1 + (S_{RM,CP} + C_{RM,CP})VD} - S_{RM,SP} \tag{32}$$

**Step 10.** (Common) Calculation of the predicted residual corneal astigmatism in power vector notation

The predicted residual corneal astigmatism is the difference between the planned and the corneal astigmatism.

The mathematical formulation is:

$$J_{0,RK} = J_{0,K} - J_{0,P} \tag{33}$$

$$J_{45,RK} = J_{45,K} - J_{45,P} \tag{34}$$

**Step 11.** (Common) Calculation of the predicted residual corneal astigmatism in clinician notation

The power vector notation is a cross-cylinder convention that is easily transposed into conventional refractions in terms of cylinder and axis in minus-cylinder or plus-cylinder formats used by clinicians.

$$C_{RK} = 2\sqrt{J_{0,RK}^2 + J_{45,RK}^2} \tag{35}$$

$$A_{RK} = \frac{\arctan\left(\frac{J_{45,RK}}{J_{0,RK}}\right)}{2} \tag{36}$$

**Step 12.** (Common) Expressing the predicted residual corneal astigmatism to keratometric astigmatism

The mathematical formulation is:

$$C_{RT} = C_{RK} \frac{n_{Topo} - n_{Air}}{n_{Cornea} - n_{Air}} \tag{37}$$

**Step 13.** Possible scenarios for planning the astigmatic correction

We have developed 5 methods to combine the information:

- a. Plan to correct the manifest astigmatism (nothing from topography)
- b. Plan to correct the corneal astigmatism (all from topography)
- c. Plan to correct a combination of manifest and corneal astigmatism, minimizing the residual global astigmatism magnitude (half the way between manifest and topographical astigmatism)
- d. Plan to correct a combination of manifest and corneal astigmatism, minimizing the magnitude of the corrected astigmatism (as much as possible from topography and manifest astigmatism without overcorrecting any of them)
- e. Plan to correct a combination of manifest and corneal astigmatism, prioritizing with-the-rule corneal astigmatism
  - a. *Plan to correct the manifest astigmatism*

To correct the manifest astigmatism represents considering nothing from the topographical astigmatism.

The mathematical formulation is:

$$M_P = M_{MR} \quad (38)$$

$$J_{0,P} = J_{0,MR} \quad (39)$$

$$J_{45,P} = J_{45,MR} \quad (40)$$

*b. Plan to correct the corneal astigmatism*

To correct the corneal astigmatism represents considering only the topographical astigmatism.

The mathematical formulation is:

$$M_P = M_K \quad (41)$$

$$J_{0,P} = J_{0,K} \quad (42)$$

$$J_{45,P} = J_{45,K} \quad (43)$$

*c. Plan to minimize the residual global astigmatism magnitude*

To correct a combination of manifest and corneal astigmatism, minimizing the residual global astigmatism magnitude represents in mathematical formulation:

$$C_{Global} = \sqrt{C_{RM}^2 + C_{RK}^2} \quad (44)$$

$$C_{Global} = 2\sqrt{J_{0,RM}^2 + J_{45,RM}^2 + J_{0,RK}^2 + J_{45,RK}^2} \quad (45)$$

$$C_{Global} = 2\sqrt{(J_{0,MR} - J_{0,P})^2 + (J_{45,MR} - J_{45,P})^2 + (J_{0,K} - J_{0,P})^2 + (J_{45,K} - J_{45,P})^2} \quad (46)$$

We should find which plan minimizes the global cylinder:

The mathematical formulation is:

$$M_P = M_{MR} \quad (47)$$

$$J_{0,P} = \frac{J_{0,MR} + J_{0,K}}{2} \quad (48)$$

$$J_{45,P} = \frac{J_{45,MR} + J_{45,K}}{2} \quad (49)$$

*d. Plan to minimize the risk of overcorrecting any of the astigmatisms*

To correct a combination of manifest and corneal astigmatism, minimizing the magnitude of the corrected astigmatism, as much as possible from topography and manifest astigmatism without overcorrecting any of them, represents in mathematical formulation:

$$M_P = M_{MR} \tag{50}$$

$$J_{0,P} = \begin{cases} J_{0,MR} < 0, J_{0,K} < 0 \Rightarrow \max(J_{0,MR}, J_{0,K}) \\ J_{0,MR} > 0, J_{0,K} > 0 \Rightarrow \min(J_{0,MR}, J_{0,K}) \\ otherwise \Rightarrow 0 \end{cases} \tag{51}$$

$$J_{45,P} = \begin{cases} J_{45,MR} < 0, J_{45,K} < 0 \Rightarrow \max(J_{45,MR}, J_{45,K}) \\ J_{45,MR} > 0, J_{45,K} > 0 \Rightarrow \min(J_{45,MR}, J_{45,K}) \\ otherwise \Rightarrow 0 \end{cases} \tag{52}$$

*e. Plan to prioritize with-the-rule corneal astigmatism*

To correct a combination of manifest and corneal astigmatism, prioritizing with-the-rule corneal astigmatism, represents in mathematical formulation:

$$M_P = M_{MR} \tag{53}$$

$$J_{0,P} = \begin{cases} J_{0,MR} < 0, J_{0,K} < 0 \Rightarrow \max(J_{0,MR}, J_{0,K}) \\ J_{0,MR} > 0, J_{0,K} > 0 \Rightarrow \min(J_{0,MR}, J_{0,K}) \\ otherwise \Rightarrow 0 \end{cases} \tag{54}$$

$$J_{45,P} = \frac{J_{45,MR} + J_{45,K}}{2} \tag{55}$$

**Step 14.** (Common) Expressing the ablation plan in clinician notation

The power vector notation is a cross-cylinder convention that is easily transposed into conventional refractions in terms of cylinder and axis in minus-cylinder or plus-cylinder formats used by clinicians.

$$S_{P,CP} = M_P - \frac{C_{P,CP}}{2} \tag{56}$$

$$C_{P,CP} = 2\sqrt{J_{0,P}^2 + J_{45,P}^2} \quad (57)$$

$$A_p = \frac{\arctan\left(\frac{J_{45,P}}{J_{0,P}}\right)}{2} \quad (58)$$

**Step 15.** (Common) Expressing the ablation plan in clinician notation at spectacle plane  
We then recalculate the correction components from the corneal plane to the spectacle plane:

$$S_{P,SP} = \frac{S_{P,CP}}{1 + S_{P,CP}VD} \quad (59)$$

$$C_{P,SP} = \frac{S_{P,CP} + C_{P,CP}}{1 + (S_{P,CP} + C_{P,CP})VD} - S_{P,SP} \quad (60)$$

The idea of corneal vs. manifest astigmatism is not new.

The difference is that the decision used to be a „all-in/no-go“ decision, either full manifest correction or full corneal astigmatism correction.

We have developed 5 methods to combine the information, from which 2 are the "most novel and interesting ones":

0. Plan to correct the manifest astigmatism (nothing from topography)
1. Plan to correct the corneal astigmatism (all from topography)
2. **Plan to correct a combination of manifest and corneal astigmatism, minimizing the residual global astigmatism magnitude (half the way between manifest and topographical astigmatism)**
3. **Plan to correct a combination of manifest and corneal astigmatism, minimizing the magnitude of the corrected astigmatism (as much as possible from topography and manifest astigmatism without overcorrecting any of them)**
4. Plan to correct a combination of manifest and corneal astigmatism, prioritizing with-the-rule corneal astigmatism

What would you do if a patient shows -1.50x170 corneal astigmatism but -1.50x10 manifest?

There are quite a number of parameters to consider:

- Vertex distance
- Different refractive indices between topographers and cornea
- Astigmatism angle
- Neural compensation
- etc...

for instance, the patient is -3.50 -1.50x10 @ 12, and Maloney indices are 43.25x80 and 41.75x170.

At first sight, we are an easy case with low astigmatisms.

Actually, the patient is -3.36 -1.36x10 @ corneal plane (-1.67 D manifest astigmatism), and Maloney are 48.18x80 and 46.51x170 (-1.67 D corneal astigmatism).

Planning the 5 scenarios:

0. Plan to correct the manifest astigmatism (-3.50 -1.50x10 @ 12)
1. Plan to correct the corneal astigmatism (-3.33 -1.85x170 @ 12)
2. Plan to correct a combination of manifest and corneal astigmatism, minimizing the residual global astigmatism magnitude (-3.46 -1.57x179 @ 12)
3. Plan to correct a combination of manifest and corneal astigmatism, minimizing the magnitude of the corrected astigmatism (-3.54 -1.41x0 @ 12)
4. Plan to correct a combination of manifest and corneal astigmatism, prioritizing with-the-rule corneal astigmatism (-3.54 -1.41x179 @ 12)

Postoperative predicted refractions would be:

0. Plan to correct the manifest astigmatism (0)
1. Plan to correct the corneal astigmatism (+0.54 -1.08x53 @ 12)
2. Plan to correct a combination of manifest and corneal astigmatism, minimizing the residual global astigmatism magnitude (+0.27 -0.54x53 @ 12)
3. Plan to correct a combination of manifest and corneal astigmatism, minimizing the magnitude of the corrected astigmatism (+0.23 -0.46x45 @ 12)
4. Plan to correct a combination of manifest and corneal astigmatism, prioritizing with-the-rule corneal astigmatism (+0.26 -0.52x45 @ 12)

And the predicted postop corneal astigmatism:

0. Plan to correct the manifest astigmatism (-0.97x143)
1. Plan to correct the corneal astigmatism (0)
2. Plan to correct a combination of manifest and corneal astigmatism, minimizing the residual global astigmatism magnitude (-0.48x143)
3. Plan to correct a combination of manifest and corneal astigmatism, minimizing the magnitude of the corrected astigmatism (-0.58x149)
4. Plan to correct a combination of manifest and corneal astigmatism, prioritizing with-the-rule corneal astigmatism (-0.53x150)

We propose 5 justified scenarios:

0. Plan to correct the manifest astigmatism (because it best satisfies patients subjective feeling)
1. Plan to correct the corneal astigmatism (because the correction is directly onto the cornea applied)
2. Plan to correct a combination of manifest and corneal astigmatism, minimizing the residual global astigmatism magnitude (because the global residual astigmatism is thereby minimised)
3. Plan to correct a combination of manifest and corneal astigmatism, minimizing the magnitude of the corrected astigmatism (because less corrected astigmatism means less tissue removed)
4. Plan to correct a combination of manifest and corneal astigmatism, prioritizing with-the-rule corneal astigmatism (because statistically with-the-rule corneal astigmatism is dominant)

## 5. Centration of refractive profiles

Not to forget the fact that astigmatism (especially high ones) has its main origin in the anterior corneal surface, and topographically is usually found located 2-fold symmetrically

from the normal corneal vertex (CV) and not at the pupil centre. Controversy remains regarding where to centre corneal refractive procedures to maximize the visual outcomes. A misplaced refractive ablation might result in undercorrection and other undesirable side effects. The coaxial light reflex seems to lie nearer to the corneal intercept of the visual axis than the pupil centre (PC) and is, thus, recommended that the corneal coaxial light reflex be centered during refractive surgery. Boxer Wachler et al.<sup>23</sup> identified the coaxial light reflex and used it as the centre of the ablation. De Ortueta and Arba Mosquera<sup>24</sup> used the corneal vertex (CV) measured by videokeratoscopy<sup>25</sup> as the morphologic reference to centre corneal refractive procedures.

Mainly, two different centration references that can be detected easily and measured with currently available technologies. PC may be the most extensively used centration method for several reasons. First, the pupil boundaries are the standard references observed by the eye-tracking devices. Moreover, the entrance pupil can be well represented by a circular or oval aperture, and these are the most common ablation areas. Centering on the pupil offers the opportunity to minimize the optical zone size. Because in LASIK there is a limited ablation area of about 9.25 mm (flap cap), the maximum allowable optical zone will be about 7.75 mm. Because laser ablation is a destructive tissue technique, and the amount of tissue removed is directly related to the ablation area diameter,<sup>26</sup> the ablation diameter, maximum ablation depth, and ablation volume should be minimized. The planned optical zone should be the same size or slightly larger as the functional entrance pupil for the patients' requirements.

The pupil centre considered for a patient who fixates properly defines the line-of-sight, which is the reference axis recommended by the OSA for representing the wavefront aberration<sup>27</sup>.

The main HOA effects (main parts of coma and spherical aberrations) arise from edge effects, i.e., strong local curvature changes from the optical zone to the transition zone and from the transition zone to the untreated cornea. It then is necessary to emphasize the use of a large optical zone (6.50 millimeter or more) to cover the scotopic pupil size, and a large and smooth transition zone.

Nevertheless, because the pupil centre is unstable, a morphologic reference is more advisable<sup>28,29,30</sup>. It is well known that the pupil centre shifts with changes in the pupil size<sup>47</sup>, moreover, because the entrance pupil we see is a virtual image of the real one.

The CV in different modalities is the other major choice as the centration reference. In perfectly acquired topography, if the human optical system were truly coaxial, the corneal vertex would represent the corneal intercept of the optical axis. Despite the fact that the human optical system is not truly coaxial, the cornea is the main refractive surface. Thus, the corneal vertex represents a stable preferable morphologic reference. However, there are several ways to determine the corneal vertex: the most extensively used one is to determine the coaxial corneal light reflex (1<sup>st</sup> Purkinje image). Nevertheless, as de Ortueta and Arba Mosquera<sup>24</sup> pointed out, there is a problem using the coaxial light reflex because surgeons differ; for instance, the coaxial light reflex will be seen differently depending on surgeon eye dominance, surgeon eye balance, or the stereopsis angle of the microscope. For example, the LadarVision platform (Alcon) uses a coaxial photograph as reference to determine the coaxial light reflex<sup>31</sup>, which is independent of the surgeons' focus. Ablations can be centered using the pupillary offset, the distance between the pupil centre and the normal CV.

If an optical zone equivalent to the maximum pupil size (scotopic pupil size or dim mesopic) is applied on the corneal vertex, due to the offset, the ablation will not cover the full pupil area and it will be cut across it. As the pupil aperture represents the only area capable of collecting light, then the full pupil should be covered and an “oversized” OZ centered on the vertex shall be selected as:

$$OZ > Pupil_{sco} + 2(\|Offset\| + \|AETAcc\|) \quad (61)$$

However, centering in the pupil with a right selected OZ is not an easy task. We know that the pupil centre shifts versus pupil size changes; moreover as the pupil we see (entrance pupil) is a virtual image of the real one.

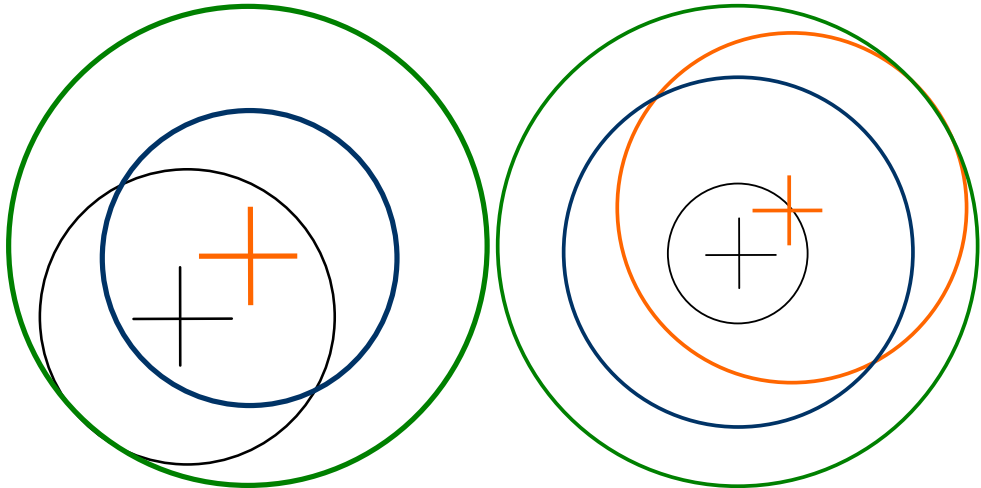


Fig. 13. **Left:** The black cross indicates the pupil centre and the black circle the maximum pupil boundaries, whereas the orange cross represents the corneal apex. Pay attention that if we apply on the corneal apex an optical zone equivalent to the maximum pupil size (scotopic pupil size or dim mesopic) (blue circle), due to the offset, the ablation will not cover the full pupil area and it will be cut across it. As the pupil aperture represents the only area capable of collecting light, then the full pupil should be covered and an “oversized” OZ centred on the apex shall be selected (green circle). **Right:** Only centring in the scotopic pupil (orange circle and cross) offers the opportunity to minimise the Optical Zone size (OZ), but under the laser pupil size is likely in a photopic state rather than dim mesopic one. Therefore, centring in the laser pupil an optical zone equivalent to the maximum pupil size (scotopic pupil size or dim mesopic) will induce edge effects.

Considering this, for aspherical, or, in general, non-wavefront-guided treatments, in which the minimum patient data set (sphere, cylinder, and axis values) from the diagnosis is used, it is assumed that the patient’s optical system is aberration-free or that those aberrations are not clinically relevant (otherwise a wavefront-guided treatment would have been planned). For those reasons, the most appropriate centering reference is the corneal vertex; modifying the corneal asphericity with an ablation profile neutral for aberrations, including loss of efficiency compensations.

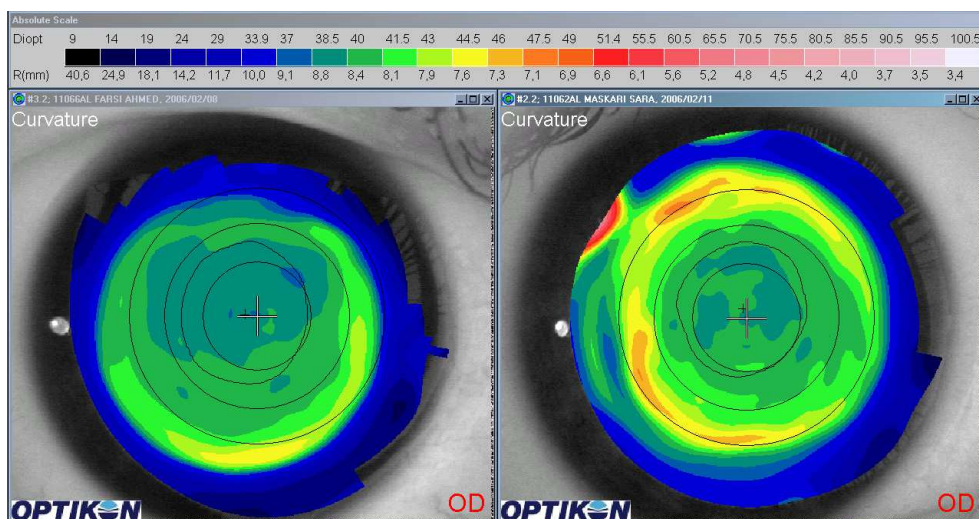


Fig. 14. Comparison of topographical findings after centration at the pupil centre and corneal vertex, respectively. Notice the more symmetric topography after CV centration.

For wavefront-guided treatments, change in aberrations according to diagnosis measurements, a more comprehensive data set from the patient diagnosis is used, including the aberrations, because the aberrations maps are described for a reference system in the centre of the entrance pupil. The most appropriate centering reference is the entrance pupil as measured in the diagnosis<sup>27</sup>.

Providing different centering references for different types of treatments is not ideal, because it is difficult to standardize the procedures. Nevertheless, ray tracing indicates that the optical axis is the ideal centering reference. Because this is difficult to standardize and considering that, the anterior corneal surface is the main refractive element of the human eye, the CV, defined as the point of maximum elevation, will be the closest reference. It shall be, however, noticed that on the less prevalent oblate corneas the point of maximum curvature (corneal apex) might be off centre and not represented by the corneal vertex.

However, it would be interesting to refer the corneal and/or ocular wavefront measurements to the optical axis or the CV. This can be done easily for corneal wavefront analysis, because there is no limitation imposed by the pupil boundaries. However, it is not as easy for ocular wavefront analysis, because the portion of the cornea above the entrance pupil alone is responsible for the foveal vision. Moreover, in patients with corneal problems such as keratoconus/keratectasia, post-LASIK (pupil-centered), corneal warpage induced by contact lens wearing and other diseases causing irregularity on anterior corneal surface, the corneal vertex and the corneal apex may shift. In those cases, pupil centre is probably more stable. Moreover, since most laser systems are designed to perform multiple procedures besides LASIK, it is more beneficial that excimer laser systems have the flexibility to choose different centration strategies.

Due to the smaller angle kappa associated with myopes compared with hyperopes<sup>32,33</sup>, centration issues are less apparent. However, angle kappa in myopes may be sufficiently



large to show differences in results, because it is always desirable to achieve as much standardization as possible and not to treat the myopes using one reference, whereas the hyperopes use a different one.

The use of large optical zones may be responsible for the lack of difference in postoperative visual outcomes using two different centration. However, hyperopic LASIK provides smaller functional optical zones and, for this reason, special caution shall be paid to these patients<sup>34</sup>.

Previous studies have reported that based on theoretical calculations with 7.0-mm pupils even for customized refractive surgery, that are much more sensitive to centration errors, it appears unlikely that optical quality would be degraded if the lateral alignment error did not exceed 0.45 mm<sup>37</sup>. In 90% of eyes, even accuracy of 0.8 mm or better would have been sufficient to achieve the goal<sup>37</sup>.

A pupillary offset of 0.25 millimeters seems to be sufficiently large to be responsible for differences in ocular aberrations<sup>28</sup>, however, not large enough to correlate this difference in ocular aberrations with functional vision.

Centering on the pupil offers the opportunity to minimize the optical zone size, whereas centering in the CV offers the opportunity to use a stable morphologic axis and to maintain the corneal morphology after treatment.

## 6. Eye-tracking

### The Cyclotorsion Problem

The analysis of cyclotorsion movements have been made since the middle of the 20<sup>th</sup> century. Several papers demonstrate some dynamic compensatory movement to keep the image at the retina aligned to a natural orientation, whereas some suggestions have been made on significant cyclotorsion occurring under monocular viewing conditions<sup>35</sup>.

Measuring rotation when the patient is upright<sup>36</sup> to when the refractive treatments are performed with the patient supine may lead to ocular cyclotorsion, resulting in mismatching of the applied versus the intended profiles<sup>37,38</sup>. Recently, some equipment can facilitate measurement of and potential compensation for static cyclotorsion occurring when the patient moves from upright to the supine position during the procedure<sup>39</sup>, quantifying the cyclorotation occurring between wavefront measurement and laser refractive surgery<sup>40</sup> and compensating for it<sup>41,42,43</sup>.

Further measuring and compensating ocular cyclotorsion during refractive treatments with the patient supine may reduce optical noise of the applied versus the intended profiles<sup>44,45,46</sup>.

It usually happens that the pupil size and centre differ for the treatment compared to that during diagnosis.<sup>47</sup> Then, excluding cyclotorsion, there is already a lateral displacement that mismatches the ablation profile. Further, cyclotorsion occurring around any position other than the ablation centre results in additional lateral displacement combined with cyclotorsion.<sup>48</sup>

Many studies, in the last times have worked out in an excellent way, the methodologies and implications of ocular cyclotorsion, but due to inherent technical problems, not many papers pay attention to the repeatability and reproducibility of the measurements.

Arba Mosquera et al.<sup>38</sup> obtained an average cyclotorsional error of 4.39°, which agrees with the observations of Ciccio et al.,<sup>49</sup> who reported 4°. However, a non-negligible percentage of

eyes may suffer cyclotorsions exceeding 10 degrees. These patients would be expected to have at least 35% residual cylinder.

Without eye registration technologies,<sup>50,51</sup> considering that maximum cyclotorsion measured from the shift from the upright to the supine position does not exceed  $\pm 14^\circ$ ,<sup>49</sup> explains why “classical” spherocylindrical corrections in refractive surgery succeed without major cyclotorsional considerations. The limited amount of astigmatism especially that can be corrected effectively for this cyclotorsional error may explain partly some unsuccessful results reported in refractive surgery.

Considering that the average cyclotorsion resulting from the shift from the upright to the supine position is about  $\pm 4^\circ$ ,<sup>49</sup> without an aid other than manual orientation, confirms why spherocylindrical corrections in laser refractive surgery have succeeded.

With currently available eye registration technologies, which provide an accuracy of about  $\pm 1.5^\circ$ , opens a new era in corneal laser refractive surgery, because patients may be treated for a wider range of refractive problems with enhanced success ratios. However, this requires a higher resolution than technically achievable with currently available systems.<sup>52,53</sup>

Bueeler and co-authors<sup>54</sup> determined conditions and tolerances for cyclotorsional accuracy. Their OT criterion represents an optical benefit condition, and their results for the tolerance limits ( $29^\circ$  for 3-mm pupils and  $21^\circ$  for 7-mm pupils) did not differ greatly from the optical benefit result for astigmatism by Arba Mosquera et al.,<sup>38</sup> confirming that astigmatism is the major component to be considered.

Cyclotorsional errors result in residual aberrations and with increasing cyclotorsional error there is a greater potential for inducing aberrations. Eyes having over  $10^\circ$  of calculated cyclotorsion, predict approximately a 35% residual astigmatic error. Because astigmatic error is generally the highest magnitude vectorial aberration, patients with higher levels of astigmatism are at higher risk of problems due to cyclotorsional error.

Ocular cyclotorsion during laser refractive surgery may lead to significant decrease in the refractive outcomes due to inadequate correction or induction of astigmatism and higher order aberrations<sup>1</sup>. During normal activities, human eyes can undergo significant torsional movements of up to 15 degrees of the resting position depending on the motion and orientation of the patient's head and body<sup>2</sup>. In particular, there can be a significant degree of cyclotorsion, particularly with monocular viewing conditions, between the seated and supine positions ranging from  $0^\circ$ – $16^\circ$  in published studies<sup>1-5</sup>. This type of cyclotorsion that occurs when the patient moves from the upright to the supine position is known as static cyclotorsion and can lead to significant unwanted outcomes during refractive laser ablations of astigmatic eyes. Theoretical analyses show that a  $4^\circ$  misalignment can lead to a 14% under-treatment of astigmatism,  $6^\circ$  to 20% under-correction and  $16^\circ$  to a 50% under-correction<sup>1</sup>.

Cyclotorsion control may be of 2 types: i) *dynamic* cyclotorsion controls that allows compensation for torsional eye movements during the laser treatments and ii) *static* cyclotorsion control that allows compensation for torsional differences in eye positions between the patient being in an upright (during diagnosis) and supine position (during surgery). Currently, new installed excimer lasers have the ability to compensate for cyclotorsion, but most of the excimer lasers in use do not have such ability.

Calculation of the static cyclotorsion is based on comparisons of the corneal wavefront image obtained from the Keratron-Scout videokeratoscope [Optikon 2000 S.p.A, Italy] from

the patient in the upright position and the image taken from the SCHWIND AMARIS laser camera with the patient in the supine position. The laser computer algorithm searches for important landmarks starting at the borderline of the pupil and moving outwards until the image is completely scanned or the number of the prerequisite important points is reached. The software algorithm scans both the iris and the sclera. Mostly the rainbow shape of the iris with the vessels in the sclera provides enough information to register the cyclotorsion and no preoperative marking of the eye is necessary. In the case of a photopic pupil size, the iris delivers more reliable data. However, if the pupil is of scotopic size and the iris is reduced to a thin ring, the structures at the sclera can be detected and used to improve the robustness of the search. Before the treatment starts the advanced cyclotorsion control algorithm of the laser compares the 2 images, superimposes the important landmarks and calculates the angle of rotation. The laser software automatically corrects for the dynamic cyclotorsion. However, the surgeon has the possibility to ask for static cyclotorsion compensation or not, with a range of compensation of  $\pm 15^\circ$ . Accuracy of cyclotorsion compensation is increased by the fact that algorithm used by the SCHWIND AMARIS does not rotate the complete volume of ablation but rather compensates each pulse individually for the cyclotorsion.

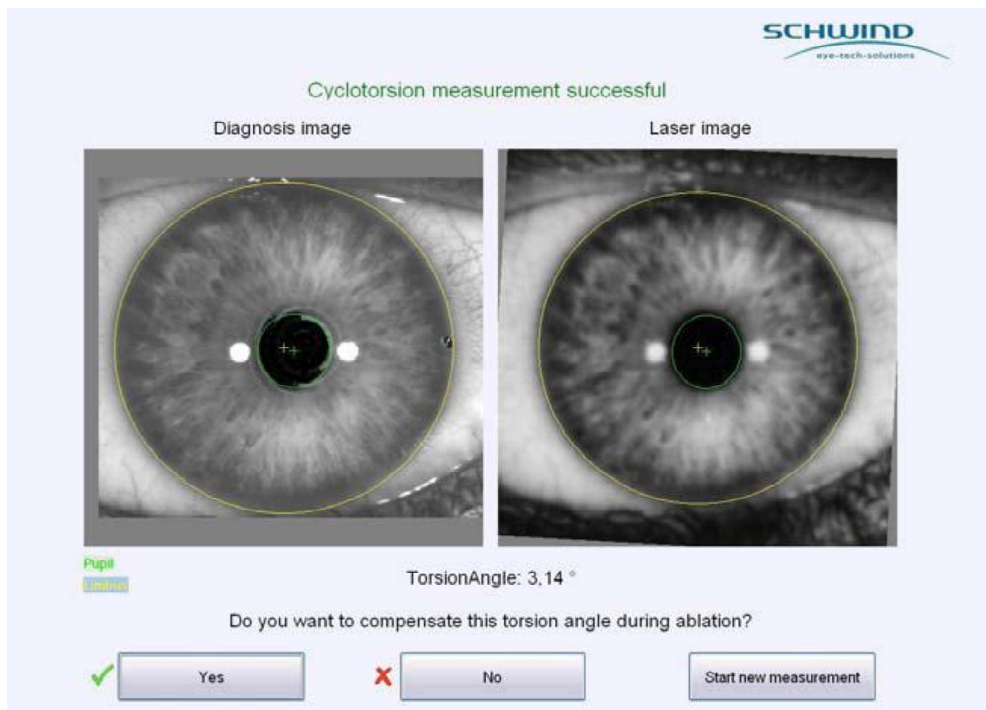


Fig. 15. SCC compensation at the AMARIS.

The amount of static cyclotorsion that occurs in individuals has ranged from 0- 16° in published studies<sup>1-5</sup>. In our experience with AMARIS, we observed a low to moderate amount of static cyclotorsion ranging from 0.3°- 10° with a mean value of 3.9°. Theoretical analyses would suggest that such an average amount of static cyclotorsion would account for a 14% under-correction of astigmatism increasing significantly with larger angles of static cyclotorsion. The static cyclotorsion module available on SCHWIND AMARIS platform produces a significant improvement in both the refractive outcome and full treatment of astigmatism. Thus we can conclude that the software is able to accurately lock on to eye position and compensate for the static cyclotorsion. This significant improvement in astigmatic and refractive outcomes in the SCC group is translated into improved safety. Noteworthy the magnitude and distribution of uncompensated cyclotorsion in former patients treated without SCC is similar to the magnitude and distribution of compensated cyclotorsion in the SCC. The importance of compensation of even small amounts of cyclotorsion would be expected to be even more important in wavefront guided treatments where it has been calculated that to achieve the diffraction limit in 95% of measured normal eyes with a 7.0 mm pupil, alignment of wavefront guided treatment would require a torsional precision of 1 degree or better<sup>11</sup>.

Not all lasers have specific software and/or hardware to actively compensate for positional cyclotorsion, and some achieve excellent results through alternative approaches. For example, Wavelight lasers achieve excellent outcomes for treatment of astigmatism. This is most likely due to the use of a lighting system which provides an "artificial horizon" which the patient sees when in the supine position under the laser.

The good thing of the SCC with CW is that the same image for topographical analysis is used for CW analysis and for SCC as well (as opposed to OW in which the H-S image is used for OW and another image, simultaneous or not, is used for SCC). The corneal wavefront image and the iris and sclera images are the same, so no mapping is needed. The Keratron keratoscope obtains information about the iris and sclera.

Uncompensated cyclotorsion errors in the SCC group can be attributed to: resolution and accuracy of the diagnosis image, resolution and accuracy of the laser image, possible misalignment of the scanner to the ET camera, possible misalignment of the manifest astigmatism to the topography, etc...

Ocular cyclotorsion during laser refractive surgery may lead to significant decrease in the refractive outcomes due to inadequate correction or induction of astigmatism and higher order aberrations, if astigmatism and higher order aberrations are present AND ONLY IF astigmatism and higher order aberrations are attempted to be corrected.

## 7. Other concerns

Tissue saving concerns

The real impact of tissue saving algorithms in customized treatments is still discussed in a controversial way. The problem of minimizing the amount of tissue is that it must be done in such a way that:

- a. does not compromise the refractive correction<sup>55,56,57,58,59</sup>
- b. does not compromise the visual performance
- c. is safe, reliable and reproducible

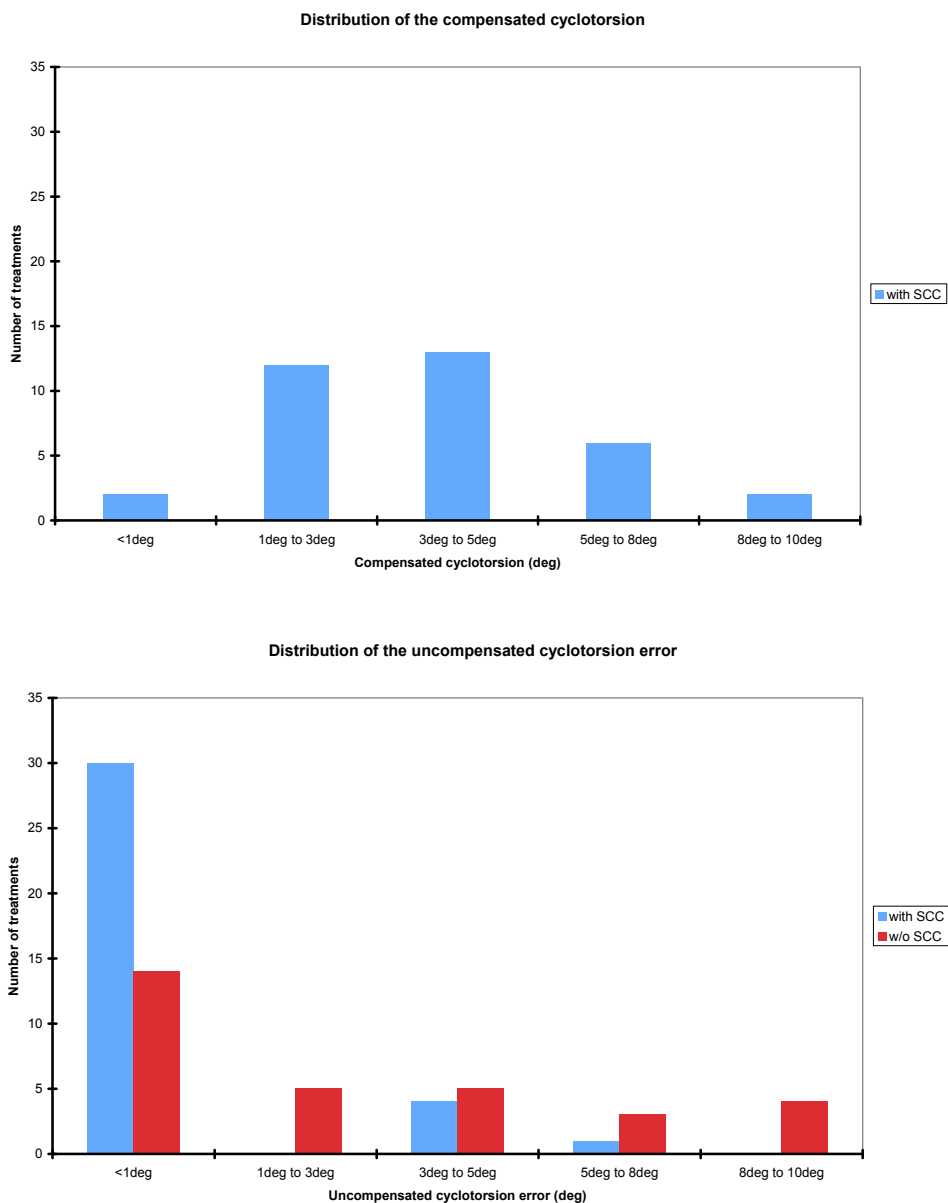


Fig. 16. Comparison of compensated (top) and uncompensated (bottom) torsional errors. Notice the similarities of the distribution of the compensated torsion when using SCC and of the uncompensated torsion when not using SCC. Notice as well, the much tighter distribution around smaller residual torsional errors for the uncompensated torsion when using SCC.

In general, for the same amount of equivalent defocus, the optical blur produced by higher order aberrations increases with increasing radial order and decreases with increasing angular frequencies. With this basis, a simple approach for classification of the clinical relevance of single aberration terms (metric for dioptric equivalence) can be proposed. It is important to bear in mind that 1 diopter of cardinal astigmatism (at  $0^\circ$  for example) does not necessarily have the same effect as 1 diopter of oblique astigmatism (at  $45^\circ$  for example). Despite this, other studies have proved this assumption as reasonable<sup>60</sup>.

According to this classification, Zernike terms can be considered not clinically relevant if their associated optical blur is lower than  $< 0.25$  D, Zernike terms that might be considered clinically relevant correspond to optical blur values between 0.25 D and 0.50 D, and Zernike terms considered clinically relevant have associated optical blur values larger than 0.50 D.

There are different proposed approaches for minimizing tissue ablation in refractive surgery:

In the multizonal treatments<sup>61</sup>, the minimization is based on the concept of progressive decreasing corrections in different optical zones. The problem comes from the induced aberrations (especially spherical aberration).

In the treatments planned with smaller optical zone<sup>62</sup> combined with bigger transition zones, the minimization is a variation of the multizone concept. The problem comes, as well, from the induced aberrations (especially spherical aberration).

In the treatments planned with smaller optical zone for the cylindrical component<sup>63</sup> (in general for the most powerful correction axis), the minimization is based upon the concept of the maximal depth being based on the lowest meridional refraction and the selected optical zone, and the effective optical zone of the highest meridional refraction is reduced to match the same maximal depth. The problem comes from the induced aberrations (especially high order astigmatism).

In the boost slider method, minimization is produced by linear modulation of the ablated volume. The problem comes from induced changes in refraction produced by modulation.

In the Z-clip method<sup>64</sup>, minimization consists of defining a "saturation depth" for the ablated volume, all points planned to ablate deeper than the saturation value are ablated only by an amount equal to the saturation value. The problem is that this "saturation limit" may occur anywhere in the ablation volume, compromising the refraction when they occur close to the ablation centre, and affecting the induction of aberrations in a complicated way.

In the Z-shift method<sup>64</sup>, minimization consists of defining a "threshold value" for the ablated volume, no points planned to ablate less than the threshold value are ablated, and the rest of the points are ablated by an amount equal to the original planned ablation minus the threshold value. The problem comes from the fact that this "threshold value" may occur anywhere in the ablation volume, compromising the refraction when they occur close to the ablation centre, and the functional optical zone when occurring at the periphery.

Other minimization approaches<sup>65</sup> consist of simplifying the profile by selecting a subset of Zernike terms that minimizes the necessary ablation depth of ablation volume but respecting the Zernike terms considered as clinically relevant.

For each combination subset of Zernike terms, the low order terms are recalculated in a way that it does not compromise the refractive correction. Considering that the Zernike terms are either planned to be corrected or left, it does not compromise the visual performance because all left (not planned to correct) terms are below clinical relevance. The proposed approaches are safe, reliable and reproducible due to the objective foundation upon which they are based. In the same way, the selected optical zone will be used for the correction.

It is important to remark; the selection of the Zernike terms to be included in the correction is not trivial. Only Zernike terms considered not clinically relevant or minor clinically relevant can be excluded from the correction, but they must not be necessarily excluded. Actually, single Zernike terms considered not clinically relevant will only be disabled when they represent an extra tissue for the ablation, and will be enabled when they help to save tissue for the ablation.

In this way, particular cases are represented by the full wavefront correction, by disabling all not clinically relevant terms, or by disabling all high order terms.

The selection process is completely automatically driven by a computer, ensuring systematic results, and minimization of the amount of tissue to be ablated, simplifying the foreseeable problems of manually selecting the adequate set of terms.

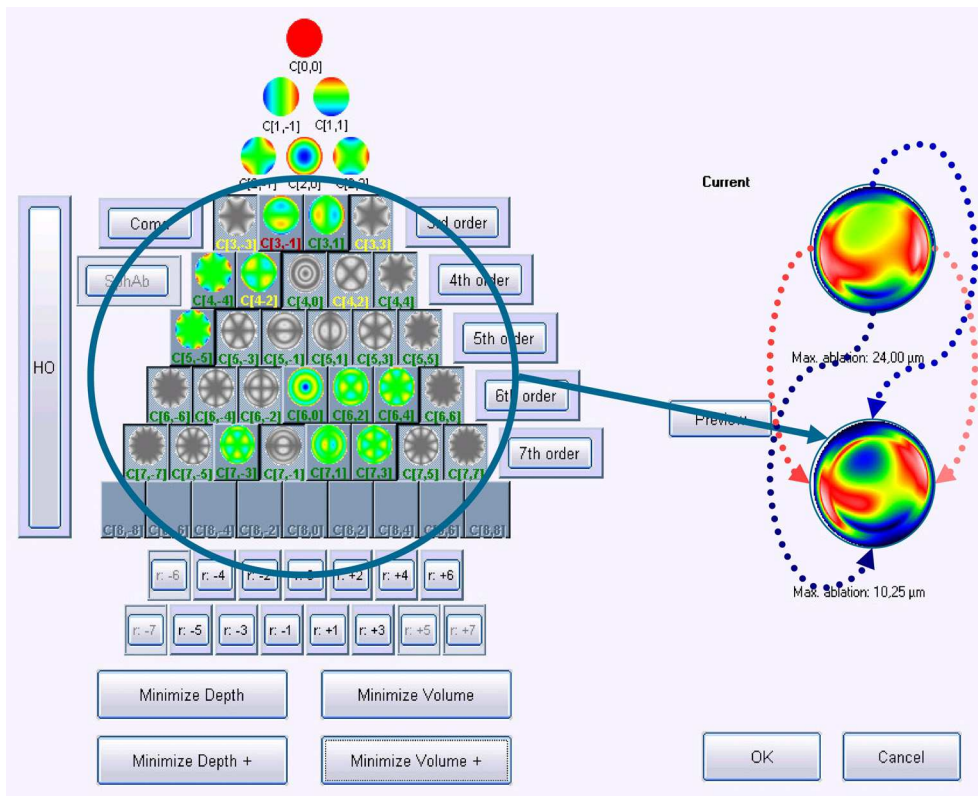


Fig. 17. Optimised Aberration Modes Selection. Based on the wavefront aberration map, the software is able to recommend the best possible aberration modes selection to minimise tissue and time, without compromising the visual quality. Notice that the wavefront aberration is analysed by the software showing the original ablation for a full wavefront correction and the suggested set of aberration modes to be corrected. Notice the difference in required tissue, but notice as well that the most representative characteristics of the wavefront map are still presented in the minimised tissue selection.

A critic to this methodology is the fact that it does not target a diffraction limited optical system. That means it reduces the ablated tissue at the cost of accepting a “trade-off” in the optical quality. However, there are, at least, three criteria (chromatic blur, depth of focus, wide field vision) favoring the target of leaving minor amounts of not clinically relevant aberrations. There are, as well, no foreseeable risks derived from the proposed minimization functions because they propose ablation profiles simpler than the full wavefront corrections. Some drawbacks and potential improvements may be hypothesized:

There may be a sort of “edge” problem considering the case that a Zernike term with DEq of 0.49 D can be enabled or disabled, due to its expected minor clinical relevance, whereas a Zernike term with DEq of 0.51 D shall be corrected.

It is controversial, as well, whether the clinical relevance of every Zernike term can be considered independently. The visual effect of an aberration does not only depend on it but also in the other possible aberration present; e.g. a sum of small, and previously considered clinically irrelevant aberration, could suppose a clear loss of overall optical quality.

A possible improvement comes from the fact that current selection strategy is in an “ON/OFF” fashion for each Zernike term, better corrections and higher amounts of tissue saving could be obtained by using a correcting factor  $F[n,m]$  (range 0 to 1) for each Zernike correcting a wavefront of the form:

$$Abl(\rho, \theta) = \sum_{n=0}^{\infty} \sum_{m=-n}^{+n} F_n^m C_n^m Z_n^m(\rho, \theta) \quad (62)$$

However, this would correspond to a much higher computation cost.

Another possible improvement would be to consider possible aberration couplings, at least, between Zernike modes of the same angular frequency as a new evaluation parameter.

New algorithms and ablation strategies for efficiently performing laser corneal refractive surgery in a customized form minimizing the amount of ablated tissue without compromising the visual quality are being developed. The availability of such profiles, potentially maximizing visual performance without increasing the factors of risk, would be of great value for the refractive surgery community and ultimately for the health and safety of the patients.

## 8. References

- [1] Chayet AS, Montes M, Gómez L, Rodríguez X, Robledo N, MacRae S. Bitoric laser in situ keratomileusis for correction of simple myopic and mixed astigmatism. *Ophthalmol.* 2001;108:303-8.
- [2] Chayet AS, Montes M, Gómez L, Rodríguez X, Robledo N, MacRae S. Bitoric laser in situ keratomileusis for correction of simple myopic and mixed astigmatism. *Ophthalmol.* 2001;108:303-8
- [3] el Danasoury MA, Waring GO 3rd, el Maghraby A, Mehrez K. Excimer laser in situ keratomileusis to correct compound myopic astigmatism. *J Refract Surg;* 1997; 13: 511-520.
- [4] Mastropasqua L, Toto L, Zuppari E, Nubile M, Carpineto P, Di Nicola M, Ballone E. Photorefractive keratectomy with aspheric profile of ablation versus conventional photorefractive keratectomy for myopia correction: six-month controlled clinical trial. *J Cataract Refract Surg;* 2006;32:109-16

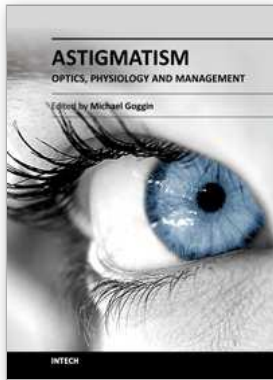


- [5] Arba Mosquera S, de Ortueta D. Geometrical analysis of the loss of ablation efficiency at non-normal incidence. *Opt. Express*; 2008; 16: 3877-3895
- [6] Accuracy of Zernike polynomials in characterizing optical aberrations and the corneal surface of the eye. Carvalho LA. *Invest Ophthalmol Vis Sci*. 2005 Jun;46(6):1915-26
- [7] Klein SA. Optimal corneal ablation for eyes with arbitrary Hartmann-Shack aberrations. *J Opt Soc Am A Opt Image Sci Vis*; 1998; 15: 2580-2588.
- [8] Kirwan C, O'Keefe M. Comparative study of higher-order aberrations after conventional laser in situ keratomileusis and laser epithelial keratomileusis for myopia using the technolas 217z laser platform. *Am J Ophthalmol*; 2009 ; 147: 77-83.
- [9] McLellan JS, Marcos S, Prieto PM, Burns SA. Imperfect optics may be the eye's defence against chromatic blur. *Nature*; 2002; 417: 174-6
- [10] Bará S, Navarro R. Wide-field compensation of monochromatic eye aberrations: expected performance and design trade-offs. *J. Opt. Soc. Am. A* 2003; 20: 1-10
- [11] Cheng X, Bradley A, Thibos LN. Predicting subjective judgment of best focus with objective image quality metrics. *J Vis*; 2004; 4: 310-321.
- [12] Marsack JD, Thibos LN, Applegate RA. Metrics of optical quality derived from wave aberrations predict visual performance. *J Vis*; 2004; 4: 322-328.
- [13] Thibos LN. Unresolved issues in the prediction of subjective refraction from wavefront aberration maps. *J Refract Surg*. 2004 Sep-Oct;20(5):S533-6.
- [14] Watson AB, Ahumada AJ Jr. Predicting visual acuity from wavefront aberrations. *J Vis*; 2008; 8: 1-19.
- [15] Marcos S, Sawides L, Gamba E, Dorransoro C. Influence of adaptive-optics ocular aberration correction on visual acuity at different luminances and contrast polarities. *J Vis*. 2008; 8: 1-12.
- [16] Salmon TO, West RW, Gasser W, Kenmore T. Measurement of refractive errors in young myopes using the COAS Shack-Hartmann aberrometer. *Optom Vis Sci*; 2003; 80: 6-14.
- [17] Chateau N, Harms F, Levecq X. Refractive representation of primary wavefront aberrations. 5th International Congress of Wavefront Sensing & Optimized Refractive Corrections; Whistler, Canada; 2004.
- [18] Bará S, Arines J, Ares J, Prado P. Direct transformation of Zernike eye aberration coefficients between scaled, rotated, and/or displaced pupils. *J Opt Soc Am A Opt Image Sci Vis*; 2006; 23: 2061-2066.
- [19] Nam J, Thibos LN, Iskander DR. Describing ocular aberrations with wavefront vergence maps. *Clin Exp Optom*; 2009; Epub ahead of print.
- [20] Applegate RA, Marsack JD, Thibos LN. Metrics of retinal image quality predict visual performance in eyes with 20/17 or better visual acuity. *Optom Vis Sci*; 2006; 83: 635-640.
- [21] Ravikumar S, Thibos LN, Bradley A. Calculation of retinal image quality for polychromatic light. *J Opt Soc Am A Opt Image Sci Vis*; 2008; 25: 2395-2407.
- [22] Hartridge H. Chromatic aberration and resolving power of the eye. *J Physiol*; 1918; 52: 175-246.
- [23] Boxer Wachler BS, Korn TS, Chandra NS, Michel FK. Decentration of the optical zone: Centering on the pupil versus the coaxially sighted corneal light reflex in LASIK for hyperopia. *J Refract Surg* 2003; 19: 464-465

- [24] de Ortueta D, Arba Mosquera S. Centration during hyperopic LASIK using the coaxial light reflex. *J Refract Surg* 2007; 23: 11
- [25] Mattioli R, Tripoli NK. Corneal Geometry Reconstruction with the Keratron Videokeratographer. *Optometry and Vision Science*; 1997; 74: 881-894.
- [26] Gatinel D, Hoang-Xuan T, Azar DT. Determination of corneal asphericity after myopia surgery with the excimer laser: a mathematical model. *Invest Ophthalmol Vis Sci* 2001; 42: 1736-1742
- [27] Thibos LN, Applegate RA, Schwiegerling JT, Webb R; VSIA Standards Taskforce Members. Vision science and its applications. Standards for reporting the optical aberrations of eyes. *J Refract Surg*. 2002; 18: S652-60
- [28] Arbelaez MC, Vidal C, Arba-Mosquera S. Clinical outcomes of corneal vertex versus central pupil references with aberration-free ablation strategies and LASIK. *Invest Ophthalmol Vis Sci*. 2008; 49: 5287-94
- [29] de Ortueta D, Schreyger FD. Centration on the cornea vertex normal during hyperopic refractive photoablation using videokeratoscopy. *J Refract Surg*. 2007; 23: 198-200
- [30] Bueeler M, Iseli HP, Jankov M, Mrochen M. Treatment-induced shifts of ocular reference axes used for measurement centration. *J Cataract Refract Surg*. 2005; 31: 1986-94
- [31] Chan CC, Boxer Wachler BS. Centration analysis of ablation over the coaxial corneal light reflex for hyperopic LASIK. *J Refract Surg*. 2006; 22: 467-71
- [32] Artal P, Benito A, Tabernero J. The human eye is an example of robust optical design. *J Vis* 2006; 6: 1-7
- [33] Tabernero J, Benito A, Alcón E, Artal P. Mechanism of compensation of aberrations in the human eye. *J Opt Soc Am A* 2007; 24: 3274-3283
- [34] Llorente L, Barbero S, Merayo J, Marcos S. Changes in corneal and total aberrations induced by LASIK surgery for hyperopia. *J Refract Surg*; 2004; 20: 203-216
- [35] Tjon-Fo-Sang MJ, de Faber JT, Kingma C, Beekhuis WH. Cyclotorsion: a possible cause of residual astigmatism in refractive surgery. *J Cataract Refract Surg*. 2002; 28: 599-602
- [36] Buehren T, Lee BJ, Collins MJ, Iskander DR. Ocular microfluctuations and videokeratoscopy. *Cornea*. 2002; 21: 346-51
- [37] Bueeler M, Mrochen M, Seiler T. Maximum permissible lateral decentration in aberration-sensing and wavefront-guided corneal ablations. *J Cataract Refract Surg* 2003; 29: 257-263
- [38] Arba Mosquera S, Merayo-Llodes J, de Ortueta D. Clinical effects of pure cyclotorsional errors during refractive surgery. *Invest Ophthalmol Vis Sci*; 2008; 49: 4828-4836
- [39] Chernyak DA. From wavefront device to laser: an alignment method for complete registration of the ablation to the cornea. *J Refract Surg*. 2005; 21: 463-8
- [40] Chernyak DA. Cyclotorsional eye motion occurring between wavefront measurement and refractive surgery. *J Cataract Refract Surg*. 2004; 30: 633-8
- [41] Bharti S, Bains HS. Active cyclotorsion error correction during LASIK for myopia and myopic astigmatism with the NIDEK EC-5000 CX III laser. *J Refract Surg*. 2007; 23: S1041-5
- [42] Kim H, Joo CK. Ocular cyclotorsion according to body position and flap creation before laser in situ keratomileusis. *J Cataract Refract Surg*. 2008; 34: 557-61

- [43] Park SH, Kim M, Joo CK. Measurement of pupil centroid shift and cyclotorsional displacement using iris registration. *Ophthalmologica*. 2009; 223: 166-71
- [44] Porter J, Yoon G, MacRae S, Pan G, Twietmeyer T, Cox IG, Williams DR. Surgeon offsets and dynamic eye movements in laser refractive surgery. *J Cataract Refract Surg*. 2005; 31: 2058-66
- [45] Hori-Komai Y, Sakai C, Toda I, Ito M, Yamamoto T, Tsubota K. Detection of cyclotorsional rotation during excimer laser ablation in LASIK. *J Refract Surg*. 2007; 23: 911-5
- [46] Chang J. Cyclotorsion during laser in situ keratomileusis. *J Cataract Refract Surg*. 2008; 34: 1720-6
- [47] Yang Y, Thompson K, Burns S. Pupil location under mesopic, photopic and pharmacologically dilated conditions. *Invest Ophthalmol Vis Sci* 2002; 43: 2508-2512
- [48] Guirao A, Williams D, Cox I. Effect of rotation and translation on the expected benefit of an ideal method to correct the eyes higher-order aberrations. *J.Opt.Soc.Am.A*;2001;18:1003-1015
- [49] Ciccio AE, Durrie DS, Stahl JE, Schwendeman F. Ocular cyclotorsion during customized laser ablation. *J Refract Surg*. 2005; 21: S772-S774
- [50] Chernyak DA. Iris-based cyclotorsional image alignment method for wavefront registration. *IEEE Transactions on Biomedical Engineering*. 2005; 52: 2032-2040.
- [51] Schruender S, Fuchs H, Spasovski S, Dankert A. Intraoperative corneal topography for image registration. *J Refract Surg* 2002; 18: S624-S629
- [52] Huang D, Arif M. Spot size and quality of scanning laser correction of higher-order wavefront aberrations. *J Cataract Refract Surg*. 2002; 28: 407-416
- [53] Guirao A, Williams D, MacRae S. Effect of beam size on the expected benefit of customized laser refractive surgery. *J Refract Surg*. 2003; 19: 15-23
- [54] Bueeler M, Mrochen M, Seiler T. Maximum permissible torsional misalignment in aberration-sensing and wavefront-guided corneal ablation. *J Cataract Refract Surg*. 2004; 30: 17-25
- [55] Cheng X, Bradley A, Thibos LN. Predicting subjective judgment of best focus with objective image quality metrics. *J Vis*; 2004; 4: 310-321.
- [56] Marsack JD, Thibos LN, Applegate RA. Metrics of optical quality derived from wave aberrations predict visual performance. *J Vis*; 2004; 4: 322-328.
- [57] Thibos LN. Unresolved issues in the prediction of subjective refraction from wavefront aberration maps. *J Refract Surg*. 2004 Sep-Oct;20(5):S533-6.
- [58] Watson AB, Ahumada AJ Jr. Predicting visual acuity from wavefront aberrations. *J Vis*; 2008; 8: 1-19.
- [59] Marcos S, Sawides L, Gamba E, Dorronsoro C. Influence of adaptive-optics ocular aberration correction on visual acuity at different luminances and contrast polarities. *J Vis*. 2008; 8: 1-12.
- [60] Remón L, Tornel M, Furlan WD. Visual Acuity in Simple Myopic Astigmatism: Influence of Cylinder Axis. *Optom Vis Sci* 2006; 83: 311-315
- [61] Kim HM, Jung HR. Multizone photorefractive keratectomy for myopia of 9 to 14 diopters. *J Refract Surg*; 1995; 11: S293-S297.

- [62] Kermani O, Schmiedt K, Oberheide U, Gerten G. Early results of nidek customized aspheric transition zones (CATz) in laser in situ keratomileusis. *J Refract Surg*; 2003; 19: S190-S194.
- [63] Kezirian GM. A Closer Look at the Options for LASIK Surgery. *Review of Ophthalmology*; 2003; 10: 12.
- [64] Goes FJ. Customized topographic repair with the new platform: ZEISS MEL80/New CRS Master TOSCA II (Chapter 18, pp. 179-193) in *Mastering the Techniques of Customised LASIK* edited by Ashok Garg and Emanuel Rosen, Jaypee Medical International (2007)
- [65] Arba Mosquera S, Merayo-Llodes J, de Ortueta D. Tissue-Saving Zernike terms selection in customised treatments for refractive surgery. *J Optom*; 2009; in press



## **Astigmatism - Optics, Physiology and Management**

Edited by Dr. Michael Goggin

ISBN 978-953-51-0230-4

Hard cover, 308 pages

**Publisher** InTech

**Published online** 29, February, 2012

**Published in print edition** February, 2012

This book explores the development, optics and physiology of astigmatism and places this knowledge in the context of modern management of this aspect of refractive error. It is written by, and aimed at, the astigmatism practitioner to assist in understanding astigmatism and its amelioration by optical and surgical techniques. It also addresses the integration of astigmatism management into the surgical approach to cataract and corneal disease including corneal transplantation.

### **How to reference**

In order to correctly reference this scholarly work, feel free to copy and paste the following:

Samuel Arba-Mosquera, Sara Padroni, Sai Kolli and Ioannis M. Aslanides (2012). Optimized Profiles for Astigmatic Refractive Surgery, *Astigmatism - Optics, Physiology and Management*, Dr. Michael Goggin (Ed.), ISBN: 978-953-51-0230-4, InTech, Available from: <http://www.intechopen.com/books/astigmatism-optics-physiology-and-management/optimized-profiles-for-astigmatic-refractive-surgery>

# **INTECH**

open science | open minds

### **InTech Europe**

University Campus STeP Ri  
Slavka Krautzeka 83/A  
51000 Rijeka, Croatia  
Phone: +385 (51) 770 447  
Fax: +385 (51) 686 166  
[www.intechopen.com](http://www.intechopen.com)

### **InTech China**

Unit 405, Office Block, Hotel Equatorial Shanghai  
No.65, Yan An Road (West), Shanghai, 200040, China  
中国上海市延安西路65号上海国际贵都大饭店办公楼405单元  
Phone: +86-21-62489820  
Fax: +86-21-62489821

© 2012 The Author(s). Licensee IntechOpen. This is an open access article distributed under the terms of the [Creative Commons Attribution 3.0 License](#), which permits unrestricted use, distribution, and reproduction in any medium, provided the original work is properly cited.